Abrupt environmental and climatic change during the deposition of the Early Permian Haushi limestone, Oman

M.H. Stephenson[1], L. Angiolini[2], M.J. Leng[3], T.S. Brewer[4], F. Berra[2], F. Jadoul[2], G. Gambacorta[2], V. Verna[2], B. Al Beloushi[5]

[1]British Geological Survey, Keyworth, Nottingham, NG12 5GG, United Kingdom

[2]Dipartimento di Scienze della Terra "A. Desio", Università degli Studi di Milano, Via Mangiagalli 34, Milano, 20133, Italy

[3]NERC Isotope Geosciences Laboratory, British Geological Survey, Keyworth, Nottingham, NG12 5GG, United Kingdom

[4]Department of Geology, University of Leicester, University Road, Leicester, LE1 7RH, United Kingdom

[5]Petroleum Development Oman, Muscat, Oman

Abstract

During the late Sakmarian (Early Permian), the Haushi limestone was deposited in a shallow embayment of the Neotethys Ocean covering what is now north Oman and parts of southeast Saudi Arabia. The sea persisted through the late Sakmarian, but by the time of the deposition of the ?Artinskian Middle Gharif Member, limestone deposition had ceased and generally arid fluvial and minor lacustrine

palaeonvironments in a low accommodation space setting had become established. Analysis of three subsurface cored boreholes and other surface sections of the Haushi limestone show an upward change in microfacies from bryonoderm to molechfor associations reflecting the passage from heterozoan to photozoan communities. The biotic turnover indicates cooler climate and eutrophy in the lower parts of the unit and an upward trend towards warmer climate and more oligotrophic conditions in the upper part. Common autochthonous algal palynomorphs and high $\delta^{13}C_{org}$ in the lower part suggest high nutrient levels were due to greater fluvial runoff, while allochthonous pollen assemblages indicate that the climate of the hinterland became more arid through the deposition of the unit, causing upward increasing seawater trends in $\delta^{18}O_{carb}$ and $\delta^{13}C_{carb}$. Several extraneous factors are likely to have contributed to this palaeoenvironmental change, which was more abrupt than in other parts of post glacial Early Permian Gondwana. First the Haushi sea, being an embayment partially isolated by Hawasina rift shoulder uplift, was more vulnerable to changes in rainfall and runoff than an open sea. Second, continued post glacial global warming and small northward movement of Gondwana may have contributed to temperature increase. Aridity may have been caused by the influence of rift shoulders to the northeast and southeast which formed barriers to humid onshore monsoon winds in the southern hemisphere summer.

Keywords: Permian, Haushi limestone, Oman, Tethys, palaeontology

Introduction

A period of climatic amelioration in the Asselian - Sakmarian lead to widespread

deglaciation following the Carboniferous-Permian glacial period (Stephenson et al., 2007), followed by the development of strong monsoonal climates (Parrish, 1995; Barron and Fawcett, 1995). Within this period, a conformable succession of lithologies from glacigene diamictites through marine sandstones and limestones to red beds and palaeosols were deposited in the Oman region. The succession has a variety of fossils and organic matter and thus offers a record of the biotic and isotopic aspects of deglaciation and subsequent climate change (Stephenson et al., 2005, 2007; Angiolini et al., in press). The response to climate change of the carbonate-dominated environment of the Haushi sea, which is the transgressive part of the succession, is known only from a few sections in the Huqf outcrop area of Oman (Angiolini et al., 2003). To understand better the sequence of palaeoenvironmental and palaeoecological events in the Haushi sea, and the magnitude and rapidity of these events in comparison with other Gondwanan post-glacial transgressive-regressive sequences, we carried out multidisciplinary study of three subsurface cored Petroleum Development Oman boreholes, Hasirah-1, Zauliyah –11 and Wafra-6, and integrated data with previous data from studies of the surface sections. Changing marine and terrestrial palaeoecology was tracked with detailed microfacies, palaeontological and palynological study, while terrestrial and marine geochemical evolution were traced with $\delta^{13}C_{org}$ (from sedimentary organic matter) and marine $\delta^{13}C_{carb}$, $\delta^{18}O_{carb}$ and $^{87}Sr/^{86}Sr$ (from brachiopods).

Geological setting

Deglaciation in the Arabian Peninsular coincided with the onset of Neotethyan seafloor spreading in the northern and eastern margins of Oman leading to the

opening of two basins: the Neotethyan Hawasina Basin to the east and the proto Indian Ocean-Batain Basin to the south (Al Belushi et al., 1996; Immenhauser et al., 2000; Angiolini et al., 2003; Fig. 1), as well the development of associated rift shoulders. In the rim basin delimited by these rift-shoulders, the interplay of local melting of glaciers and tectonic subsidence in the early Sakmarian lead to the widespread deposition of mudstone formed in deglacial lakes covering areas of Oman and Saudi Arabia. The largest of these was the 'Rahab lake' which covered most of southern Oman (Osterloff et al., 2004a). Following this in Oman, the marginal marine clastic sediments of the Lower Gharif Member were deposited, culminating in the deposition of the 'maximum flooding shale' of Guit et al. (1995) which corresponds to the P10 stratigraphic surface of Sharland et al. (2001), and to widespread sea level rise (Stephenson et al., 2005). In most of Oman, the 'maximum flooding shale' is marked by a unique palynological assemblage containing the acritarch *Ulanisphaeridium omanensis* (Stephenson et al., 2003). In south Oman, the facies containing the acritarch are shoreface sandstones and lagoonal claystones. Above this are facies that suggest alternation between marine and non-marine conditions up to the base of the Middle Gharif Member. In north Oman, the maximum flooding shale is succeeded by the informally-named Haushi limestone (Angiolini et al., 2006).

The distribution of the Haushi limestone suggests that at its greatest extent in the late Sakmarian, the Haushi sea covered most of north Oman and parts of southeast Saudi Arabia (Konert et al., 2001). Its southwestern extent was controlled by rising elevation and the presence of clastic sediment input. To the south, the Huqf axis was a high, with the result that Lower Permian sediments thin onto it (Fig. 1). The facies characteristics of the Haushi limestone in the area indicate highly proximal

conditions (Angiolini et al., 2006). Thus the southern edge of the Haushi sea was at or very close to the Huqf axis. To the east, the Haushi limestone is absent in the Oman mountains due either to erosion or non-deposition related to the rise of the Hawasina Basin rift shoulder in the position of the present Oman mountains in the Early Permian (Blendinger et al., 1990; Osterloff et al., 2004b). To the northeast, the Haushi limestone is present in southern Saudi Arabian wells, but knowledge of its distribution elsewhere in Saudi Arabia is poor due to low density well coverage.

The Haushi sea, being fully marine, must have been sourced from Tethyan waters but the position of ingress of marine water is unknown. The inflow is unlikely to have come from the west or northwest because of the configuration of Gondwana at the time (Fig. 1). It is also unlikely to have come from the south due to the presence of the Huqf axis. The Neotethys Ocean was closest to the east and ingress may have been through a gap in the Hawasina Basin rift shoulder in the present position of the Oman Mountains, or directly from the north through the present territory of the United Arab Emirates. The Haushi sea persisted through the late Sakmarian. By the time of the deposition of the Middle Gharif Member, limestone deposition had ceased and red fluvial, lacustrine and palaeosol facies were deposited in a low accommodation space setting (Immenhauser et al., 2000; Osterloff et al., 2004b).

The term Haushi limestone is used only in the subsurface. The equivalent lithostratigraphic unit in outcrop is the Saiwan Formation, described by Angiolini et al. (2003, 2004) from surface sections at Gharif, Saiwan and the Haushi Ring (Fig. 2A). At the type-section at Saiwan, it consists of coarse-grained, cross-laminated bioclastic sandstones, red and green mudrocks, and sandy calcarenites passing upward

to coarse-grained and cross-laminated sandy calcarenites, bioclastic limestones, and marlstones (Fig. 2A,B).

Between 100 and 150 km to the west of the surface sections, the subsurface Haushi limestone is penetrated in Hasirah-1, Zauliyah –11 and Wafra-6 wells (Figs. 2B-5). The Haushi limestone is made up of four units that reflect a shallowing-upward trend. In ascending order the units are: an interbedded bioclastic limestone and shale (unit 1); shale and sandstone (unit 2); oolitic limestone (unit 3); and finely laminated siltstone (unit 4; Angiolini et al., 2006; Figs. 3-5). These are succeeded by the non-marine shales, sandstones and palaeosols of the Middle Gharif Member.

Angiolini et al. (2006) showed that the brachiopod biozones of the Saiwan Formation can be recognised in subsurface cored borehole sections of the Haushi limestone (Fig. 2B). A late Sakmarian age is suggested for both units based chiefly on fusulinids (Angiolini et al., 2006).

Evolution of the Haushi sea

The methods used in analysis for palaeontological and palynological study are given by Angiolini et al. (2006) and Stephenson et al. (2003), and those for $\delta^{13}C_{org}$, $\delta^{13}C_{carb}$, $\delta^{18}O_{carb}$ and $^{87}Sr/^{86}Sr$ by Stephenson et al. (2005) and Angiolini et al. (in press). Quantitative analyses of the carbonate microfacies defined the compositional variation of bioclastic content in the well sections and its palaeoenvironmental significance. Thin sections from 150 samples were described; out of these, 44 thin sections were selected for point-count analysis, 23 from Wafra-6, 14 from Zauliyah-11 and 7 from Hasirah-1. Nine groups of skeletal grains (brachiopods, bryozoans, echinoderms,

gastropods, fusulinids, other foraminifers, encrusting organisms and ostracods) were identified, and three hundred points were counted in each thin section.

Microfacies

Cluster analysis was performed on the microfacies point-count data displayed in Figures 3, 4 and 5, using Cluster 3.0 by Ko Van Huissteden. The data were reduced to a matrix of 9 skeletal grain categories from 44 samples and then processed by cluster analyses in Q and R modes. Seven clusters were identified; for each cluster the average composition was calculated, as well as the standard deviation (Fig. 6). This allowed identification of the distribution of the skeletal grain type associations within the well sections (Fig. 7). Clusters 1, 2 and 4 are typical bryonoderm grain associations (Beauchamp, 1994; see Fig. 8), being characterized by brachiopods, bryozoans and echinoderms (mainly crinoids), together with minor calcareous algae. Clusters 1, 2 and 4 are present in unit 1 in Hasirah-1 and Zaulyiah-11 wells (cluster 1) and in Wafra-6 well (clusters 2 and 4). The difference in the clusters is mainly related to the variation in abundance of brachiopods and bryozoans. Cluster 5 can also be classified as bryonoderm and occurs in Zauliyah-11 and Wafra-6 wells. These clusters (1, 2, 4 and 5) occur also at the base of unit 3, indicating the persistence of a bryonoderm association after the terrigenous input represented by unit 2. The upper part of unit 3 is characterized by the presence of cluster 3 (Wafra-6) and 7 (Zauliyah-11 and Hasirah-1 wells), clearly enriched in molluscs. Clusters 3 and 7 can be interpreted as molechfor assemblages (Carannante et al., 1988; see Fig. 8), despite the fact that foraminifera are more numerous in cluster 7 (most of the encrusting forms in cluster 3 are probably encrusting foraminifera). Cluster 6 comprises the fusulinid

limestones of Wafra-6; the presence of bryozoans, brachiopods and crinoids indicate that this association can be assigned to a 'bryonoderm-extended' association (Fig. 8).

The bryonoderm grain association of unit 1 was probably deposited between fair weather and storm wave base (see Table 1). In Wafra-6, and less extensively in Hasirah-1, the 'bryonoderm-extended' high-energy fusulinid grainstones occur intermittently within the bryonoderm microfacies in unit 1. Most of the fusulinid bioclasts are reworked, suggesting long residence time on a sea-bottom swept by currents, likely above the fair weather wave-base (Table 1), probably recording a short-term environmental change in water depth or temperature. The bryonoderm association of unit 1 is succeeded by clastic sediments of unit 2 (Fig. 7), that probably record terrestrial clastic sediment input fed by erosion of a granitoid source rock since quartz, K-feldspar and mica are common. The bryonoderm association reappears at the base of the upper carbonate unit (unit 3), and it is succeeded upward by a molechfor grain association. This upper part of unit 3 is characterized by oolites, absent from the rest of the Haushi limestone, which suggests that the grain association type of this unit is not a pure molechfor, but probably a transition toward a chloroforam grain association (Beauchamp, 1994). Sediment textures indicate deposition in a relatively high-energy environment; the sea-bottom was swept by currents and was likely above fair weather wave base.

Marine biotic change

The macrofossil (mainly brachiopod) assemblages display changes similar to those of the microfacies, for example there is a sharp turnover throughout the three well sections that mirrors the change in grain association type from bryonoderm to

molechfor (Figs. 3-5). This turnover cannot simply be related to terrigenous clastic sediment input (unit 2) interrupting carbonate sedimentation, because the sedimentological and lithological features of units 1 and 3 indicate a similar depositional environment. Furthermore the major marine biotic change occurs within unit 3, after the return to carbonate sedimentation. Detailed analysis of the relative abundance of taxa together with systematic description of the brachiopod associations allows identification of the factors controlling the biotic change in the Haushi limestone.

In the Hasirah-1 well section (Fig. 3), lophophorates (brachiopods and bryozoans) have a peak of abundance in unit 1, then decrease in unit 2 and are absent from unit 3. A similar trend is shown by the echinoderms and by encrusting organisms which are rather constant from the base up to the lower part of unit 3 and then disappear. By contrast, molluscs are very rare in the lower two units and increase sharply where lophophorates decrease. Ostracods also show a peak of abundance in the upper part of unit 3. Zauliyah-11 records a similar trend (Fig. 5) with molluscs increasing from the base of the oolitic limestones in parallel with a decrease of lophophorates and echinoderms. The peak in abundance of ostracods occurs at the same level as a peak in microforaminifers.

Wafra-6 shows a complex multiphase pattern in unit 1, with two distinct peaks of abundance of the lophophorates (Fig. 4), the lower one given both by brachiopods and bryozoans and the upper chiefly by brachiopods. Above these two peaks there is a rapid and episodic biotic change suggested by the presence of intensely-reworked fusulinid grainstones. After this short decline, lophophorates increase to reach a peak

at the base of the unit 3 and then decrease rapidly. This is mirrored by a rapid increase in molluscs and encrusting organisms. Echinoderms are more abundant in the lower part of the succession, where they show rapid change in abundance not always in phase with lophophorates; however they are still present in unit 3, in contrast with their distribution in other well sections.

The biotic change through the Haushi limestones in the three sections mainly reflects the passage from heterozoan to photozoan assemblages (Table 1) and may be related to depth, temperature, nutrient availability and salinity fluctuations (e.g. Beauchamp and Baud, 2002; Reid et al., 2007). Overall the succession records a shallowing upward trend from water depths between fair weather and storm wave base in unit 1 to water depths above fair weather wave base in units 3 and 4, but this trend is not sufficient to produce a significant biotic turnover, as Early Permian lophophorates are widespread also at shallow depths.

Similarly, the change from heterozoan to photozoan communities cannot be ascribed merely to sea-level fall as we would expect to record the presence of photozoan elements exported from shallow to deeper water to be deposited inside the heterozoan dominated sediments. Photozoan grains are not observed in the bryonoderm microfacies, suggesting that during their deposition no photozoan was present at shallower depth.

Temperature increased between the deposition of the diamictites of the Al Khlata Formation and unit 1 of the Haushi limestone because warm climate photozoan fusulinids occur in the upper part of that unit (e.g. in Wafra-6; Fig. 4, Table 1), but it is difficult to quantify the warming trend within the Haushi limestone itself.

However, the presence of photozoan forms and the synchronous decrease in heterozoan organisms is more likely reflect a change from cold to temperate conditions. Furthermore, this warming trend is confirmed by the occurrence in unit 3 of ooids, which according to James (1997) only form in warm water.

Temperature may not be the sole control on the observed biotic change, because nutrient availability has also proved to be important in other similar environments (e.g. Reid et al., 2007). Thus the upward decrease of lophophorates through the three sections can be also be explained by variation in nutrient supply (Table 1). Lophophorates usually dominate in high nutrient environments and large spire-bearing brachiopods, are particularly well-adapted to such conditions (Perez-Huerta and Sheldon, 2006). Overall high nutrient levels with fluctuations in nutrient supply may have been responsible for the sharp variations in lophophorate abundance observed in unit 1 in the Wafra-6 section. Among lophophorates, the brachiopods are represented by large spire-bearing genera.

Nutrient supply probably continued to fluctuate in the upper part of unit 1. This is suggested by the localised abundance of photozoan fusulinids in parallel with a rapid decline in lophophorates. Large fusiform foraminifers of the type in the Haushi limestone probably contained photosymbionts and can thus be considered a proxy for episodes of low nutrient supply (Brasier, 1995, Reid et al., 2007). Molluscs thrive with lower and more constant nutrient supply. Thus these palaeoenvironmental conditions probably characterised unit 3.

Variation in echinoderm abundance in unit 1, as well as the widespread accumulation of heterozoan-dominated sediments at this level, suggest salinity fluctuations. This

is supported by palynological and isotopic evidence presented later. In Hasirah-1 and Zauliyah-11, a change in salinity accompanied the decrease in nutrients during the deposition of unit 3, as echinoderms disappeared and only molluscs and ostracods proliferated.

The biotic turnover through the Haushi limestone thus suggests a general increase in temperature and a change from high but fluctuating nutrient availability in units 1 and 2 to a decrease of nutrient supply in unit 3, likely coupled with changes in salinity.

Palynology

The most common taxa in Hasirah-1, Zauliyah-11 and Wafra-6 are indeterminate bisaccate pollen (probably mainly poorly preserved specimens of *Alisporites indarraensis* Segroves, 1969)*, Vesicaspora* spp., *Kingiacolpites subcircularis* Tiwari and Moiz, 1971, *Corisaccites alutas* Venkatachala and Kar, 1966 (or Cf. *C. alutas*) and *Florinites flaccidus* Menéndez and Azcuy, 1973 (Figs. 3-5, 10-11). The main trend of terrestrially-derived allochthonous palynomorphs is the appearance and upward increase in the colpate pollen *K. subcircularis* and the bitaeniate pollen grain *C. alutas* from unit 3. *Corisaccites alutas* is similar in morphology to the bitaeniate pollen *Lueckisporites virkkiae*, which has been found in association with plants of likely xerophytic aspect that probably grew in arid conditions (Visscher, 1971; Looy, 2007). Thus the thick exine of these distinctive pollen is likely to be protection against dry conditions. *Kingiacolpites subcircularis* was probably produced by a cycad-like plant, and modern cycads, though wide in their colonisation of terrestrial habitats, tend to concentrate in dry, warm climates (Norstog and Nicholls, 1997). The overall dominance of bisaccate gymnosperm pollen (involved in water-independent

reproduction), rarity of fern spores (water-dependent propagules) as well as the upward increase of *K. subcircularis* and *C. alutas* therefore suggests a dry climate for the terrestrial hinterland of the Haushi sea, particularly those parts represented by unit 3 and 4.

Autochthonous algal palynomorphs, consisting mainly of small (<50 μ), non haptotypic, smooth-walled spheres are most common in shales interbedded with limestones in units 1 and 2 (Figs. 3-5, 10-11), and isotopic evidence presented later suggests that these may indicate lower-than-normal salinity conditions. The shales also lack acanthomorphic acritarchs (phytoplankton). Thus their intercalation with limestones containing brachiopods and echinoderms, which are unequivocally marine in origin, suggests alternation between normal and low salinity.

Isotopes

$\delta^{13}C_{org}$

The $\delta^{13}C_{org}$ of organic matter of the subsurface sections shows wide variation between approximately –20‰ and –31‰, with the majority of samples yielding values between –22‰ and –24‰. Stephenson et al. (2005) and Foster et al. (1997) showed that a strong influence on bulk $\delta^{13}C_{org}$ in mixed marine-terrestrial sections is the proportion of marine to terrestrially-derived organic matter. Studies in the Permian show that marine organic matter has low $\delta^{13}C_{org}$ (–28 to –30‰, e.g. Foster et al. 1997) while terrestrially derived organic matter (mainly wood) has high $\delta^{13}C$ (–22 to –24‰, Foster et al., 1997; Strauss and Peters-Kottig, 2003; Peters-Kottig et al., 2006). Most of the samples taken for $\delta^{13}C_{org}$ were from shales and sandstones and the generally

high values suggest that much of the organic material in those lithologies is of terrestrial plant origin, a finding consistent with studies of the coeval clastic Lower Gharif Member in south Oman (Stephenson et al., 2005). This suggests that the shale that is interbedded with limestone in units 1 and 2 was deposited either in (1) full salinity marine conditions but with little marine organic matter preserved; or more likely (2) lower-than-normal salinity such that marine low $\delta^{13}C_{org}$ was not produced. In most of the sections, the highest $\delta^{13}C_{org}$ values (–22 to –23‰) correspond with palynological assemblages containing common algal palynomorphs. A similar relationship was found in samples in the Thuleilat-16 and -42 wells in south Oman where assemblages containing very common unequivocal zygnemataceaen (fresh or brackish water) algal spores gave high $\delta^{13}C_{org}$ values of –20 to –21‰ (Stephenson et al. 2005). Thus the distribution of algal spores and $\delta^{13}C_{org}$ may indicate rapid cyclic alternation between normal marine salinity and lower salinity in units 1 and 3. This may be due to fluctuating fluvial freshwater input.

Isotopes from brachiopods

The preservation state and degree of diagenetic alteration of 130 articulate brachiopods from Wafra-6, Hasirah-1 and Zauliyah-11 was investigated using ultrastructural scanning electron microscopy and cathodoluminescence (Figs. 12 and 13). To integrate previous data from the Saiwan surface section (Angiolini et al. in press) comparisons were made of brachiopod isotopes from the same biozone, since it was not possible to identify lithological units 1 to 4 in the surface section (Fig. 9). Fifty-three specimens of the species *Neospirifer* (*Quadrospira*) aff. *hardmani* (Foord, 1890) and *Derbya haroubi* Angiolini in Angiolini et al., 1997 were considered

suitable for geochemical and isotopic analyses (Fig. 9). These pristine brachiopods were mainly from Wafra-6 well section from the *spinosa- permixta* and *hardmani-haroubi* brachiopod biozones and have $\delta^{13}C_{carb}$ between +3.2 to +5‰ and $\delta^{18}O_{carb}$ between –3.3 to –0.4‰. These values lie within the range of Permian seawater values (Korte et al., 2005) and are broadly consistent with those recorded at the surface in the same biozones (Angiolini et al., in press; Fig. 9).

Differences in the shape of the curves in Wafra-6 and the Saiwan section are due to different sampling densities, particularly in the lower part of the *spinosa- permixta* biozone. Due to this sampling effect, the basal 1-1.5‰ positive excursion in $\delta^{13}C_{carb}$ and $\delta^{18}O_{carb}$ values is thus recorded only in Wafra-6 and correlates with the first peak of abundance of lophophorates and a minor decline of echinoderms (Fig. 4). It may be linked to environmental perturbations, such as rapid variation of salinity and nutrient supply (see previous discussion).

A general increase in $\delta^{18}O_{carb}$ from values of –3.3‰ in the lower biozone to a high of –0.4‰ in the upper biozone is probably related to increasing aridity and higher evaporation causing $\delta^{18}O_{carb}$ of the Haushi sea to rise (Figure 9; Angiolini et al., in press). $\delta^{13}C$ variation between +3.2 and +5‰ is consistent with other studies for Tethyan seawater of the Early Permian (Korte et al. 2005). However, above the oscillation recorded at the base, values increase slightly. This trend is clearer at the surface, where slightly heavier $\delta^{13}C$ values are interpreted as related to increasing aridity, isolation of the Haushi sea and decreasing nutrients (Angiolini et al., in press).

$^{87}Sr/^{86}Sr$ values from Wafra-6 well section are very close to those from the equivalent

part of the Saiwan section, and both are similar to the values for the seawater curve of Korte et al. (2006) for the Sakmarian. The $^{87}Sr/^{86}Sr$ curve at the Saiwan section shows a sharp decrease in radiogenic strontium from the *omanensis* brachiopod biozone (not recorded in the subsurface) to the *spinosa- permixta* biozone, followed by more or less constant values upward (Fig. 8). The sharp decrease at the base correlates with the end of the deglaciation and can be explained by reduced riverine ^{87}Sr flux to the Haushi Basin (Angiolini et al., in press).

Discussion

The Haushi limestone occurs within a sequence of lithological units that indicate abrupt palaeoenvironmental change. The lowest unit, the Al Khlata Formation, is unequivocally glacigene (Braakman et al., 1982; Levell et al., 1988; Al-Belushi et al., 1996), characterised by diamictites and shales with dropstones. The upper subdivision of the Al Khlata Formation, the Rahab Member, is interpreted to have been deposited in a large freshwater lake of glacial meltwater (Levell et al., 1988; Wopfner, 1999; Stephenson and Osterloff, 2002). Above this are a variety of facies within the Lower Gharif Member: in north Oman are the carbonates of the Haushi limestone discussed here, while in the south are intercalated clastic marine and fluvial sediments. Capping the Lower Gharif Member are the often red fluvial, lacustrine and palaeosols facies of the Middle Gharif Member. The sequence from the glacigene facies to the red bed facies is essentially continuous with no evidence for major regional unconformity, and rarely exceeds 50m in thickness (Osterloff et al., 2004b), thus change must have occurred abruptly. The short-lived epicontinental sea that is represented by the Haushi

limestone evolved rapidly as part of this sequence of change.

This study has shown a consistent microfacies change through the Haushi limestone from bryonoderm at the base to molechfor (with some transitional features toward a chloroforam type) at the top, as well as biotic turnover related to warming and decreasing nutrient supply. Higher but fluctuating nutrients are indicated in the lower part (units 1, 2 and the base of 3), whereas low and stable nutrient supply are suggested in units 3 and 4, coupled with local changes in salinity (higher salinity according to isotopes). The presence of common autochthonous algal palynomorphs and high $\delta^{13}C_{org}$ in units 1 and 2 indicate that higher nutrients at these lower levels may have been due to greater fluvial runoff. The composition of allochthonous pollen assemblages indicate that the climate of the hinterland became more arid. High evaporation may have caused higher seawater $\delta^{18}O_{carb}$. Similarly, higher $\delta^{13}C$ values are interpreted as related to increasing aridity, isolation of the Haushi sea and decreasing nutrients.

Several extraneous factors are likely to have contributed to this rapid palaeoenvironmental change both within the period of deposition of the Haushi sea and within the longer period of change from glacial to fully arid conditions. The Haushi sea was deposited in an embayment (Konert et al., 2001) and thus was susceptible to changes in rainfall and runoff. It is also likely that the Hawasina rift shoulder rising in the east in the Sakmarian limited circulation between the Haushi sea and the Neotethys Ocean (Angiolini et al., 2003) exacerbating its isolation. However, probably more important, are the evolving climates of the Early Permian and the northward drift of Arabia in this period (e.g. Torsvik and Cocks, 2004), which appear

to have brought about a more abrupt postglacial change than that experienced in higher latitude Gondwana areas.

This difference in postglacial change is shown by recent palynological correlation of the upper Al Khlata Formation and Lower Gharif Member with sequences in southwestern Australia (Stephenson in press; Stephenson et al. in press). It shows that southwestern Australian glacigene and immediately-postglacial units (e.g. the Stockton Formation) correlate with the upper Al Khlata Formation and Rahab Member. However, stratigraphically higher units such as the Collie Coal Measures (interpreted to have been deposited in cool, wet climates; e.g. Hobday, 1987) correlate with the relatively warm, dry conditions represented by the Lower Gharif Member and the Haushi limestone. Large parts of Gondwana experienced cool, wet coal-forming environments directly after deglaciation (Isbell et al., 2003), such that Veevers and Tewari (1995) referred to the period as 'Coal Deposition 1' and the gap between it and the Late Triassic coal forming period as the 'Coal gap'. Thus the Lower Gharif Member and Haushi limestone sequence is unusual. Other areas that did not experience post-glacial coal formation include parts of central Africa, northern Australia, the panthalassan margin basins of South America (Veevers and Tewari, 1995; Isbell et al., 2003) and blocks of the Peri-Gondwanan fringe (Angiolini et al., 2005). The relatively low palaeolatitude northern Brazilian Solimões, Amazonas and Paranaíba basins experienced very little glacial activity, with Carboniferous-Permian rocks being characterized by aeolian sandstones and evaporites (Milani and Zalán, 1999). The Oman Basin, which during the Sakmarian was positioned at a latitude approximately half way between the northern Brazilian (~20°S) and the southwestern

Australian basins (~60°S; Ziegler et al., 1998), perhaps illustrates characteristics between these two extremes.

The Earth warmed in the early Sakmarian following glaciation (e.g. Isbell et al., 2003; Stephenson et al., 2007) but it seems likely that in Oman, most of this warming was complete by the time of the deposition of the Rahab Member since no diamictites occur above this level. Conditions were also already warm at the time of the deposition of the lower part of the Haushi limestone, since it contains fusulinids. Pangea moved steadily northward about 10° of latitude between the Asselian and the Middle Permian (Ziegler et al., 1998), so the movement during the - probably rapid - deposition of the Haushi limestone itself was likely very small. Thus the result of these two small contributions was that temperature increase during the deposition of the Haushi limestone was probably small. The strong effects that are seen in the Haushi limestone were perhaps, therefore, due to a combination of increasing aridity and warming.

The increase in aridity is more difficult to explain. Roscher and Schneider (2006) described an overall 'aridisation trend' in northern Pangea (mainly palaeoequatorial European basins) between the Westphalian and Middle Permian which they attributed to decreasing humidity related to the closure of the Rheic Ocean, and to the development of cold, along-coast currents on the northwestern Pangean margin, preventing onshore humid winds. There may also have been an Asselian cold current on the southwestern side of the Tethys adjacent to Oman (Angiolini et al., 2007; see also Shi and Grunt, 2000; Weldon and Shi, 2003), which could have lead to coastal aridity but this had probably disappeared by the late Sakmarian since its cause was

likely linked to nearby ice masses.

Parrish (1995) and Barron and Fawcett (1995) also showed that an intense monsoonal climate caused by the arrangement of large continental masses could contribute to palaeoequatorial aridity. Parrish (1995) suggested that as the drift northward of Pangea proceeded through the Permian, the presence of an increasingly larger land mass to the north of the equator would stimulate cross-equatorial flow and longitudinal heat transport, as is observed in the modern summer monsoon in Asia. Thus palaeoequatorial Pangea would undergo aridisation progressively from the west to the east, as well as increasingly seasonal rainfall in the coastal Tethyan regions. The western palaeoequatorial Tethys would also become arid because of the diversion and disruption of equatorial easterlies north or south into the summer hemisphere (Parrish, 1995). However, the changes in palaeoequatorial Pangea do not adequately explain the increasing aridity in the Haushi sea area because its palaeolatitude, even in the latest Sakmarian is likely to have been around 40°S (Ziegler et al., 1998).

Perhaps the most plausible explanation for postglacial aridity in the Oman area relates to the likely presence of rift shoulders to the east and south of the Haushi sea (Blendinger et al., 1990; Immenhouser et al., 2000; Angiolini et al., 2003). The elevation of the shoulders is unknown but that of the eastern Hawasina shoulder may have been considerable in view of the absence of probably several thousand metres of post Precambrian rocks beneath the Middle Permian Saiq Formation in the present day Oman Mountains (see also Angiolini et al., 2003). In southern hemisphere summer, the intertropical convergence zone (ITCZ) would have moved south and intense low pressure in the Gondwana continent interior (Parrish, 1995) would

combine to produce northeasterly trade winds or onshore monsoon winds originating in the Tethys, presumably bringing rain to the coastal areas of the Hawasina rift shoulder, but rain shadow in the basin behind. In the southern hemisphere winter either southeast trade winds would dominate in which case rain would fall preferentially on the southern Batain rift shoulder, or intense high pressure in the Gondwana continent interior would encourage strong offshore monsoon winds carrying very little water vapour to the basin. Thus in both summer and winter, rainfall would be low.

Conclusions

1. Analysis of three subsurface cored boreholes of the Haushi limestone in Oman shows an upward change in microfacies from bryonoderm to molechfor associations, and accompanying biotic turnover indicates cooler climate and eutrophy in the lower parts of the unit and an upward trend towards warmer climate and more oligotrophic conditions in the upper part.

2. Common autochthonous algal palynomorphs and high $\delta^{13}C_{org}$ in the lower part suggest high nutrient levels were due to greater fluvial runoff, while allochthonous pollen assemblages indicate that the climate of the hinterland became more arid through the deposition of the unit, also causing upward-increasing seawater trends in $\delta^{18}O_{carb}$ and $\delta^{13}C_{carb}$.

3. This palaeoenvironmental change is continued into the arid palaeoenvironments represented by the Middle Gharif Member and is more abrupt than in other parts of post glacial Early Permian Gondwana, because

over most of the continent, glacigene sediments are succeeded by cold-climate Gondwana coal facies. This may have been partly due to the Haushi sea being an embayment partially isolated by Hawasina rift shoulder uplift, and thus more vulnerable to changes in rainfall and runoff than an open sea. Though post-glacial global warming and northward movement of Gondwana may have contributed to temperature increase, aridity is more likely to have been caused by the influence of rift shoulders to the east and south and to the onset of Permian monsoon conditions.

Acknowledgements

The management of Petroleum Development Oman and the Ministry of Oil and Gas of the Sultanate of Oman are acknowledged for giving permission to publish this work. Dr Alan Heward kindly allowed access to PDO cores. M.H. Stephenson and M.J. Leng publish with the permission of the Director of the Britsish Geological Survey (NERC).

References

Al-Belushi, J.D., Glennie, K.W., Williams, B.P.J., 1996. Permo-Carboniferous glaciogenic Al Khlata Formation, Oman: a new hypothesis for origin of its glaciation. GeoArabia 1, 389-404.

Angiolini, L., Brunton, H., Gaetani, M, 2005. Early Permian (Asselian) brachiopods from Karakorum and their palaeobiogeographical significance. Palaeontology 48, 1-18.

Angiolini, L., Stephenson, M.H., Leven, Y., 2006. Correlation of the Lower Permian surface Saiwan Formation and subsurface Haushi Limestone, central Oman. GeoArabia 11, 17-38.

Angiolini, L., Balini, M., Garzanti, E., Nicora, A., Tintori, A., 2003. Gondwanan deglaciation and opening of Neotethys: the Al Khlata and Saiwan formations of interior Oman. Palaeogeography, Palaeoclimatology, Palaeoecology 196, 99-123.

Angiolini L., Crasquin-Soleau S., Platel J.-P., Roger J., Vachard D., Vaslet D., Al Husseini M., 2004. Saiwan, Gharif and Khuff formations, Haushi-Huqf Uplift, Oman. In: Al-Husseini, M.I. (Ed.), Carboniferous, Permian and Triassic Arabian Stratigraphy. GeoArabia Special Publication 3, Gulf PetroLink, Manama, Bahrain, 149-183.

Angiolini, L., Gaetani, M., Garzanti, E., Mattei, M., Muttoni, G., Stephenson, M.H., Zanchi, A., 2007. Tethyan oceanic currents and climate gradients 300 m.y. ago. Geology 35, 1071-1074.

Angiolini, L., Darbyshire, D.P.F., Stephenson, M.H., Leng, M.J., Brewer, T.S., Berra, F., Jadoul, F. Lower Permian brachiopods from Oman: their potential as climatic proxies. Transactions of the Royal Society of Edinburgh, in press.

Barron, E.J., Fawcett, P.J., 1995. The Climate of Pangaea: a review of climate model simulations of the Permian. In: Scholle, P.A., Peryt, T.M., Ulmer-Scholle, D.S. (Eds.) The Permian of Northern Pangea Vol. 1. Palaeogeography, Palaeoclimates, Stratigraphy. Springer Verlag, pp. 37- 52.

Beauchamp, B., 1994. Permian climatic cooling in the Candian Arctic. Geological Society of America Special Publication 288, Boulder, Colorado, pp. 299-246,

Beauchamp, B., Baud, A., 2002. Growth and demise of Permian biogenic chert along northwest Pangea: evidence for end-Permian collapse of thermohaline circulation. Palaeogeography, Palaeoclimatology, Palaeoecology 184, 37–63.

Blendinger, W., Van Vliet, A., Hughes Clarke, M.W., 1990. Updoming, rifting and continental margin development during the Late Palaeozoic in northern Oman. In: Robertson, A.H.F., Searle, M.P., Ries, A.C., (Eds.). The geology and tectonics of the Oman region, Geological Society of London, Special Publication 49, pp. 27-37.

Braakman, J., Levell, B., Martin, J., Potter, T. L., Van Vliet, A., 1982. Late Palaeozoic Gondwana glaciation in Oman. Nature 299, 48-50.

Brasier, M.D. 1995. Fossils as indicators of nutrient levels. 2: Evolution and extinction in relation to oligotrophy. In: Bosence D.W.J, Allison P.A. (Eds.) Marine Palaeoenvironmental Analysis from Fossils. Geological Society Special Publication 83, 133-150.

Carannante, G., Esteban, M., Milliman, J.D., Simone, L., 1988. Carbonate lithofacies as paleolatitude indicators: problems and limitations. In: Nelson, C.S. (Ed.), Non-tropical shelf carbonates - modern and ancient. Sedimentary Geology 60, 333-346.

Foster, C.B., Logan, G.A., Summons, R.E., Gorter, J.D., Edwards, D.S. 1997. Carbon isotopes, kerogen types and the Permian-Triassic boundary in Australia: implications for exploration. Australian Petroleum Production and Exploration Association

Journal, 1997, 472-489.

Guit, F.A., Al-Lawati, M.H., Nederlof, P.J.R., 1995. Seeking new potential in the Early-Late Permian Gharif play, west Central Oman. In: Al-Husseini, M.I. (Ed.) Middle East Petroleum Geosciences, GEO '94. Gulf Petrolink, Bahrain, pp. 447-462.

Hobday, D.K., 1987. Gondwana coal basins of Australia and South Africa: tectonic setting, depositional systems and resources. In: Scott, A.C. (Ed.) Coal and coal-bearing strata: recent advances. Geological Society Special Publication 32, The Geological Society, London, pp. 219-235.

Immenhauser, A., Schreurs, G., Gnos, E., Oterdoom, H.W., Hartmann, B., 2000. Late Palaeozoic to Neogene geodynamic evolution of the northeastern Oman margin. Geological Magazine 137, 1-18.

Isbell, J.L., Miller, M.F., Wolfe, K.L., Lenaker, P.A. 2003. Timing of late Paleozoic glaciation in Gondwana: was glaciation responsible for the development of northern hemisphere cyclothems? Geological Society of America Special Paper 370, 5-24.

James, N.P., 1997. The cool-water carbonate depositional realm. In: James, N.P., Clarke, J.A.D. (Eds.), Cool-water carbonates. SEPM Special Publication, vol. 56, pp. 1–23.

Konert, G., Abdulkader, M.A., Al-Hajri, S.A., Droste, H.J., 2001. Paleozoic stratigraphy and hydrocarbon habitat of the Arabian Plate. GeoArabia 6, 407-442.

Korte, C. Jasper, T., Kozur, H.W., Veizer, J., 2005. $\delta^{18}O$ and $\delta^{13}C$ of Permian

brachiopods: A record of seawater evolution and continental glaciation. Palaeogeography, Palaeoclimatology, Palaeoecology 224, 333-351.

Korte, C., Jasper, T., Kozur, H.W., Veizer, J., 2006. $^{87}Sr/^{86}Sr$ record of Permian seawater. Palaeogeography, Palaeoclimatology, Palaeoecology 240, 89-107

Levell, B.K., Braakman, J.H., Rutten, K.W., 1988. Oil-bearing sediments of Gondwana glaciation in Oman. American Association of Petroleum Geologists Bulletin 72, 775-796.

Looy, C.V., 2007. Extending the range of derived Late Paleozoic conifers: *Lebowskia* gen. nov. (Majonicaceae). International Journal of Plant Sciences 168, 957-972.

Milani, E.J., Zalán, P.V., 1999. An outline of the geology and petroleum systems of the Paleozoic interior basins of South America. Episodes 22, 199-205.

Norstog, K.J., Nicholls, T.J., 1997. Biology of Cycads. Cornell University Press, Ithaca.

Osterloff, P.L., Penney, R.A., Aitken, J., Clark, N., Al-Husseini, M.I., 2004a. Depositional sequences of the Al Khlata Formation, subsurface Interior Oman. In: Al-Husseini, M.I. (Ed.), Carboniferous, Permian and Early Triassic Arabian Stratigraphy. GeoArabia Special Publication 3, Gulf PetroLink, Manama, Bahrain, pp. 61-81.

Osterloff, P.L., Al-Harthy, A., Penney, R.A., Spaak, P., Al-Zadjali, F., Jones, N.S., Knox, R.W.O'B, Stephenson, M.H., Oliver, G., Al-Husseini, M.I., 2004b. Gharif and Khuff formations, subsurface Interior Oman. In: Al-Husseini, M.I. (Ed.), Carboniferous, Permian and Early Triassic Arabian stratigraphy, GeoArabia Special

Publication 3, Gulf PetroLink, Manama, Bahrain, pp. 83-147.

Parrish, J.T., 1995. Geological evidence of Permian climate. In: Scholle, P.A., Peryt, T. M., Ulmer-Scholle, D.S. (Eds.) The Permian of Northern Pangea Vol. 1. Palaeogeography, Palaeoclimates, Stratigraphy. Springer Verlag, pp. 53-61.

Perez Huerta, A., Sheldon, N.D., 2006. Pennsylvanian sea level cycles, nutrient availability and brachiopod paleoecology. Palaeogeography, Palaeoclimatology, Palaeoecology 230, 264– 279.

Peters-Kottig, W. Strauss, H., Kerp, H., 2006. The land plant $\delta^{13}C$ record and plant evolution in the Late Palaeozoic. Palaeogeography, Palaeoclimatology, Palaeoecology 240, 237-252.

Reid, C.M., James, N.P., Beauchamp, B., Keyser T.K., 2007. Faunal turnover and changing oceanography: Late Palaeozoic warm-to-cool water carbonates, Sverdrup Basin, Canadian Arctic Archipelago. Palaeogeography, Palaeoclimatology, Palaeoecology 249, 128-159.

Roscher, M., Schneider, J.W., 2006. Permo-Carboniferous climate: Early Pennsylvanian to Late Permian climate development of central Europe in a regional and global context. In: Lucas, S.G., Cassinis, G., Schneider, J.W. (Eds.), Non-marine Permian biostratigraphy and biochronology. Geological Society, London, Special Publications, 265, 95-136.

Sharland, P.R., Archer, R., Casey, D.M., Davies, R.B., Hall, S.H. Heward, A.P. Horbury, A.D., Simmons, M.D., 2001. Arabian Plate Sequence Stratigraphy.

GeoArabia Special Publication 2, Gulf Petrolink, Bahrain, 371p.

Shi, G.R., Grunt, T.A., 2000. Permian Gondwana - Boreal antitropicality with special reference to brachiopod faunas. Palaeogeography, Palaeoclimatology, Palaeoecology 155, 239-263.

Stephenson, M.H., in press. A review of the palynostratigraphy of Gondwanan Pennsylvanian to Lower Permian glacigene successions. In: Fielding, C.R., Frank, T.D., Isbell, J.L. (Eds.), Resolving the Late Paleozoic Ice Age in Time and Space. Geological Society of America Memoir.

Stephenson, M.H., Osterloff, P.L., 2002. Palynology of the deglaciation sequence represented by the Lower Permian Rahab and Lower Gharif members, Oman. American Association of Stratigraphic Palynologists Contribution Series 40, 1-32.

Stephenson, M.H., Osterloff, P.L., Filatoff, J. 2003. Integrated palynological biozonation of the Permian of Saudi Arabia and Oman: progress and problems. GeoArabia 8, 467-496.

Stephenson, M.H., Al Rawahi, A., Casey, B., in press. Correlation of the Al Khlata Formation in the Mukhaizna Field, Oman, based on a new downhole, cuttings-based palynostratigraphic scheme. GeoArabia.

Stephenson, M.H., Angiolini, L., Leng, M.J., 2007. The Early Permian fossil record of Gondwana and its relationship to deglaciation: a review. In: Williams, M., Haywood, A.M., Gregory, F.J., Schmidt, D.N. (Eds.), Deep-Time Perspectives on Climate Change: Marrying the Signal from Computer Models and Biological Proxies. The

Micropalaeontological Society, Special Publications. The Geological Society, London, 103–122.

Stephenson, M.H, Leng, M.J., Vane, C.H., Osterloff, P. L., Arrowsmith, C., 2005. Investigating the record of Permian climate change from argillaceous sediments, Oman. Journal of the Geological Society, London 162, 641-651.

Strauss, H., Peters-Kottig, W., 2003. The Paleozoic to Mesozoic carbon cycle revisited: the carbon isotopic composition of terrestrial organic matter. Geochemistry, Geophysics, Geosystems 4, Article Number 10, 1-15.

Torsvik, T.H., Cocks, R.M., 2004, Earth geography from 400 to 250 Ma: a palaeomagnetic, faunal and facies review. Journal of the Geological Society of London 161, 555-572.

Veevers, J.J., Tewari, R.C., 1995. Gondwana master basin of Peninsular India between Tethys and the interior of the Gondwanaland Province of Pangea, Boulder, Colorado, Geological Society of America Memoir 187, 72pp.

Visscher, H., 1971. The Permian and Triassic of the Kingscourt Outlier, Ireland. Geological Survey of Ireland Special Paper No. 1, p. 1-114.

Weldon, E.A., Shi, G.R. 2003. Global distribution of *Terrakea* Booker, 1930 (Productina Brachiopoda): implications for Permian marine biogeography and Eurasia – Gondwana correlations. XV International Congress on Carboniferous and Permian Stratigraphy. Utrecht, 2003, Abstract 583.

Wopfner, H., 1999. The Early Permian deglaciation event between East Africa and

northwestern Australia. Journal of African Earth Sciences 29, 77-90.

Ziegler, A.M., Gibbs, M.T., Hulver, M.L., 1998. A mini-atlas of oceanic water masses in the Permian period. Proceedings of the Royal Society of Victoria 110, 323-343.

Figure captions

Fig. 1. Palaeogeography of the Tethys Ocean in the Early Permian, after Angiolini et al. (2005) and Immenhauser et al. (2000).

Fig. 2. A, Location of well sections and surface sections. B, Correlation of Haushi limestone from surface to subsurface. Line of section shown in A.

Fig. 3. Lithology, selected palynomorphs, $\delta^{13}C_{org}$, microfacies (including lophophorate total), brachiopod biozones (after Angiolini et al. 2006) and electric logs for Hasirah-1 well section.

Fig. 4. Lithology, selected palynomorphs, $\delta^{13}C_{org}$, microfacies (including lophophorate total), brachiopod biozones (after Angiolini et al. 2006) and electric logs for Wafra-6 well section. Hard.-haro = *hardmani- haroubi* Biozone.

Fig. 5. Lithology, selected palynomorphs, $\delta^{13}C_{org}$, microfacies (including lophophorate total), brachiopod biozones (after Angiolini et al 2006) and electric logs for Zauliyah-11 well section.

Fig. 6. Cluster analysis of the quantitative composition of microfacies. On the right is the average composition of each cluster (bars represent standard deviation).

Fig. 7. Stratigraphic occurrence of grain association types in the three well sections, together with the distribution of clusters (see Fig. 6 for the average composition of each cluster).

Fig. 8. Microfacies, scale bar is the same for all microphotographs. a, sample Ha1-4, cluster 1, bryonoderm. Crinoids, bryozoans and brachiopods common. b, sample WA 6-2, cluster 2, bryonoderm. Bryozoans are less common than in cluster 1. c, sample WA 6-15.16, cluster 3, molechfor. Note the abundance of small reworked gastropods, associated with bivalves and foraminifera. d, WA6-8, cluster 4, bryonoderm. Brachiopods are the most common type of skeletal grain. e, f, ZL11-1.2, cluster 5, bryonoderm. Similar to d, but bryozoans are more abundant and associated with echinoderms (f: in polarized light). g, WA6-10.1, cluster 6, 'bryonoderm extended'. Reworked fusulinids abundant; brachiopods and crinoids common. h, HA1-6.4, cluster 7, molechfor. Bivalves and foramifera are common. Note the presence of oolites often with quartz at the nucleus.

Fig. 9. Comparison of $\delta^{13}C_{\text{carbonate}}$ $\delta^{18}O_{\text{carbonate}}$ and $^{87}Sr/^{86}Sr$ for Wafra-6 well section and the surface Saiwan section.

Fig. 10. Palynomorphs from Lower Gharif Member, including the Haushi limestone. The locations of specimens are given first by England Finder reference and then by slide code. All slides are held in the Micropalaeontology Collection of Petroleum Development Oman, PO Box 81, Muscat 113, Sultanate of Oman. Magnifications are approximate. a, 'Large *Leiosphaeridia* sp. 1', x 300, J44/1, 1906,2, Wafra-6. b, 'Large *Leiosphaeridia* sp. 1', x 300, M45, 1906,2, Wafra-6. c, 'Large *Leiosphaeridia* sp. 1', x 300, V50/2, 1906,2, Wafra-6. d, *Peroaletes* sp. B, x 500, C55/1, 1906,73, Wafra-

6. e, *Peroaletes* sp. B, x 500, H47, 1906,73, Wafra-6. f, Cf *Corisaccites alutas* Venkatachala and Kar, 1966, x300, E55, 1906,73, Wafra-6. g, *Vesicaspora* sp. X 500, P45/3, 1906,73, Wafra-6. h, *Striatopodocarpites fusus* (Balme and Hennelly) Potonié, 1958, x 250, E54, 8715, Hasirah-1. i, *Corisaccites alutas* Venkatachala and Kar, 1966, x 300, V54/1, 1906,73, Wafra-6. j, *Corisaccites alutas* Venkatachala and Kar,1966, x 300, N60, 1906.73, Wafra-6. k, *Lundbladispora gracilis* Stephenson and Osterloff, 2002, x 300, J53, 1911, Wafra-6. l, *Cyclogranisporites pox* Stephenson and Osterloff, 2002, x 700, E42/2, 8715, Hasirah-1. m, *Striatopodocarpites fusus* (Balme and Hennelly) Potonié, 1958, x 250, U44, 8715, Hasirah-1. n, *Lundbladispora gracilis* Stephenson and Osterloff, 2002, x 300, L46, 8704, Hasirah-1. o, *Leiosphaeridia* sp. 2, x 500, M45, 8603, Hasirah-1.

Fig. 11. a, *Leiosphaeridia* sp. 2, x 500, K42/1, 8603, Hasirah-1. b, *Leiosphaeridia* sp. 2, x 500, W59/2, 8603, Hasirah-1. c, *Leiosphaeridia* sp. 1, x 500, H5, 2465,5, Zauliyah-11. d, *Leiosphaeridia* sp. 1, x 500, G34/3, 2465,5, Zauliyah-11. e, *Leiosphaeridia* sp. 1, x 500, F51/3, 2465,5, Zauliyah-11. f, *Leiosphaeridia* sp. 1, x 500, G11/3, 2465,5, Zauliyah-11. g, *Leiosphaeridia* sp. 1, x 500, J11/3, 2465,5, Zauliyah-11. h, *Kingiacolpites subcircularis* Tiwari and Moiz ,1971, x 500, Q49, 1906,2, Wafra-6. i, *Kingiacolpites subcircularis* Tiwari and Moiz ,1971, x 500, J55/4, 1906,2, Wafra-6. j, *Florinites flaccidus* Menéndez and Azcuy, 1973, x 200, H51/2, 1906,73, Wafra-6. k, *Brevitriletes cornutus* (Balme and Hennelly) Backhouse, 1991, x 600, H5, 9733,5, Saih Rawl-8. l, *Alisporites indarraensis* Segroves, 1969, x 500, W59/2, 9733,5, Saih Rawl -8. m, *Alisporites indarraensis* Segroves, 1969, x 500, J53, 9733,5, Saih Rawl -8.

Fig. 12. SEM photomicrographs of the ultrastructure of brachiopods of the Haushi limestone. Specimens are held in the collection of the Dipartimento di Scienze della Terra "A. Desio", Università degli Studi di Milano, Via Mangiagalli 34, Milano, 20133, Italy. a, Transverse section showing the keel and saddle profile of very well preserved calcitic fibres in *Neospirifer (Quadrospira)* aff. *hardmani* (Foord, 1890), specimen WA6-1.8-3 (T), Wafra-6 well. b, Longitudinal section of thin and elongated secondary layer fibres in *Neospirifer (Quadrospira)* aff. *hardmani* (Foord, 1890), specimen ZL11-2.6-1b, Zauilyah-11 well. c, Longitudinal section of well preserved thin and elongated secondary fibres in *Neospirifer (Quadrospira)* aff. *hardmani* (Foord, 1890), specimen ZL11-2-5, Zauilyah-11 well. d, Transverse section showing the keel and saddle profile of very well preserved calcitic fibres in *Neospirifer (Quadrospira)* aff. *hardmani* (Foord, 1890), specimen ZL11-1, Zauilyah-11 well. e, Punctae deflecting well preserved fibres in *Punctocyrtella spinosa* Plodowski, 1968, specimen WA6-1-2, Wafra-6 well. f, Pseudopuncta deflecting well preserved fibres in *Derbya haroubi* Angiolini in Angiolini et al., 1997, specimen WA6-1.1-4, Wafra-6 well. g, Longitudinal section of well preserved lamellae in *Derbya haroubi* Angiolini in Angiolini et al., 1997, specimen ZL11-5-9, Zauilyah-11 well. h, Longitudinal section of well preserved lamellae, in *Derbya haroubi* Angiolini in Angiolini et al., 1997, specimen ZL11-2-15, Zauilyah-11 well.

Fig. 13. a, Cathodoluminescence photomicrograph of a non-luminescent brachiopod shell, *Neospirifer* (*Quadrospira*) aff. *hardmani* (Foord, 1890), specimen WA6-9.2-1, Wafra-6 well. b, Cathodoluminescence photomicrograph of a non-luminescent brachiopod shell, *Derbya haroubi* Angiolini in Angiolini et al., 1997, specimen WA6-9.2-2, Wafra-6 well. c, Cathodoluminescence photomicrograph of a luminescent

1 brachiopod shell, *Reedoconcha permixta* (Reed, 1932), specimen WA6-7-2, Wafra-6
2 well.

3 **Table 1**. Environmental significance of skeletal grains in the carbonate microfacies in
4 relation to feeding strategy, nutrient sensitivity, approximate water depth and
5 preferred substrate.

Figure 1

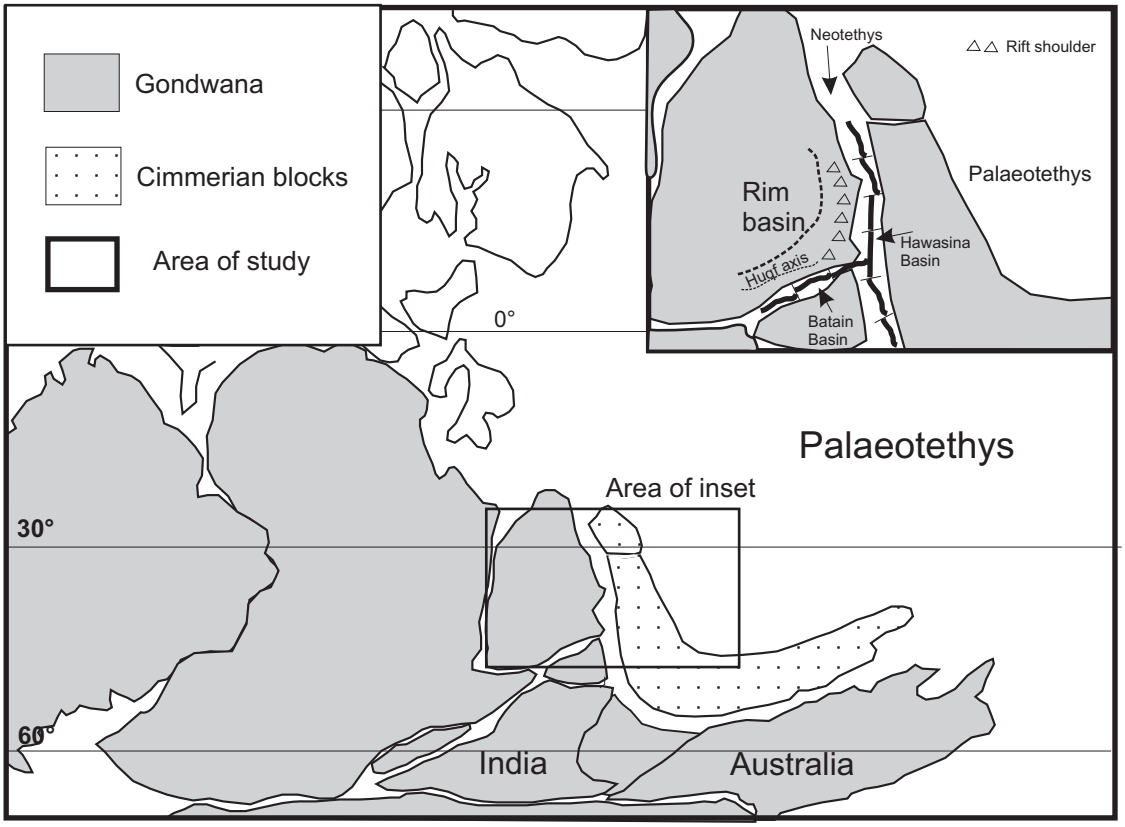

Fig 1

Figure 2

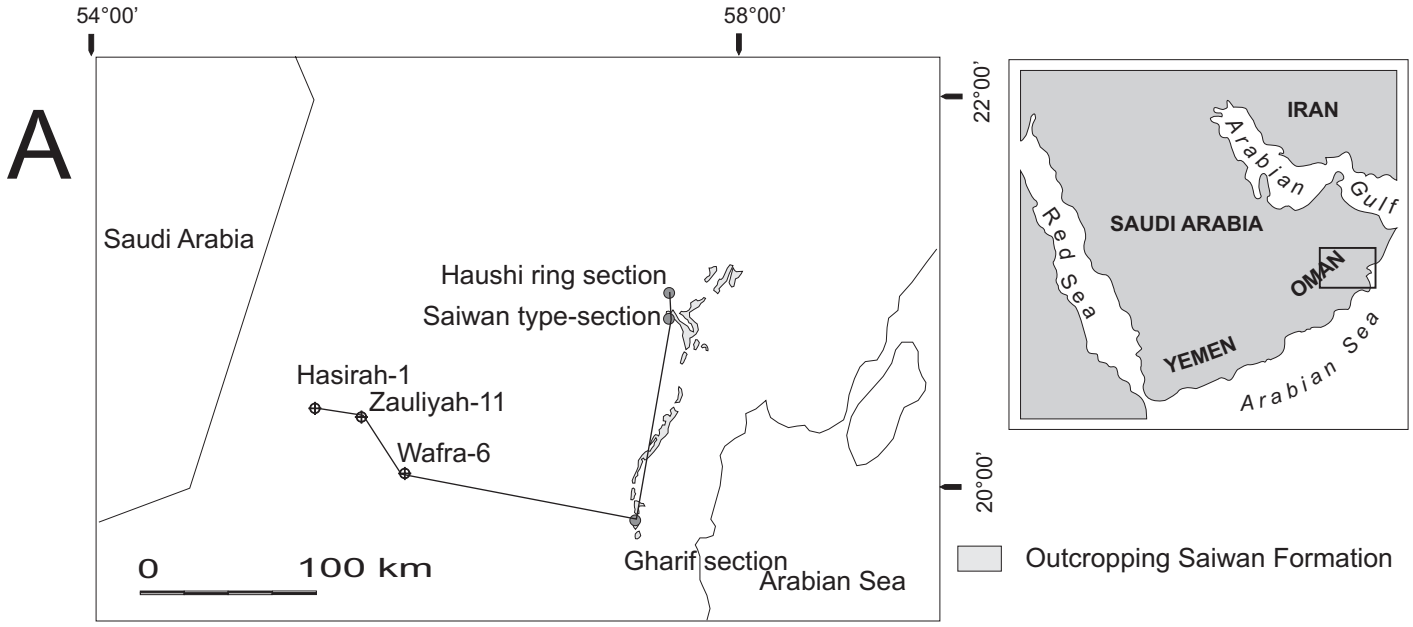

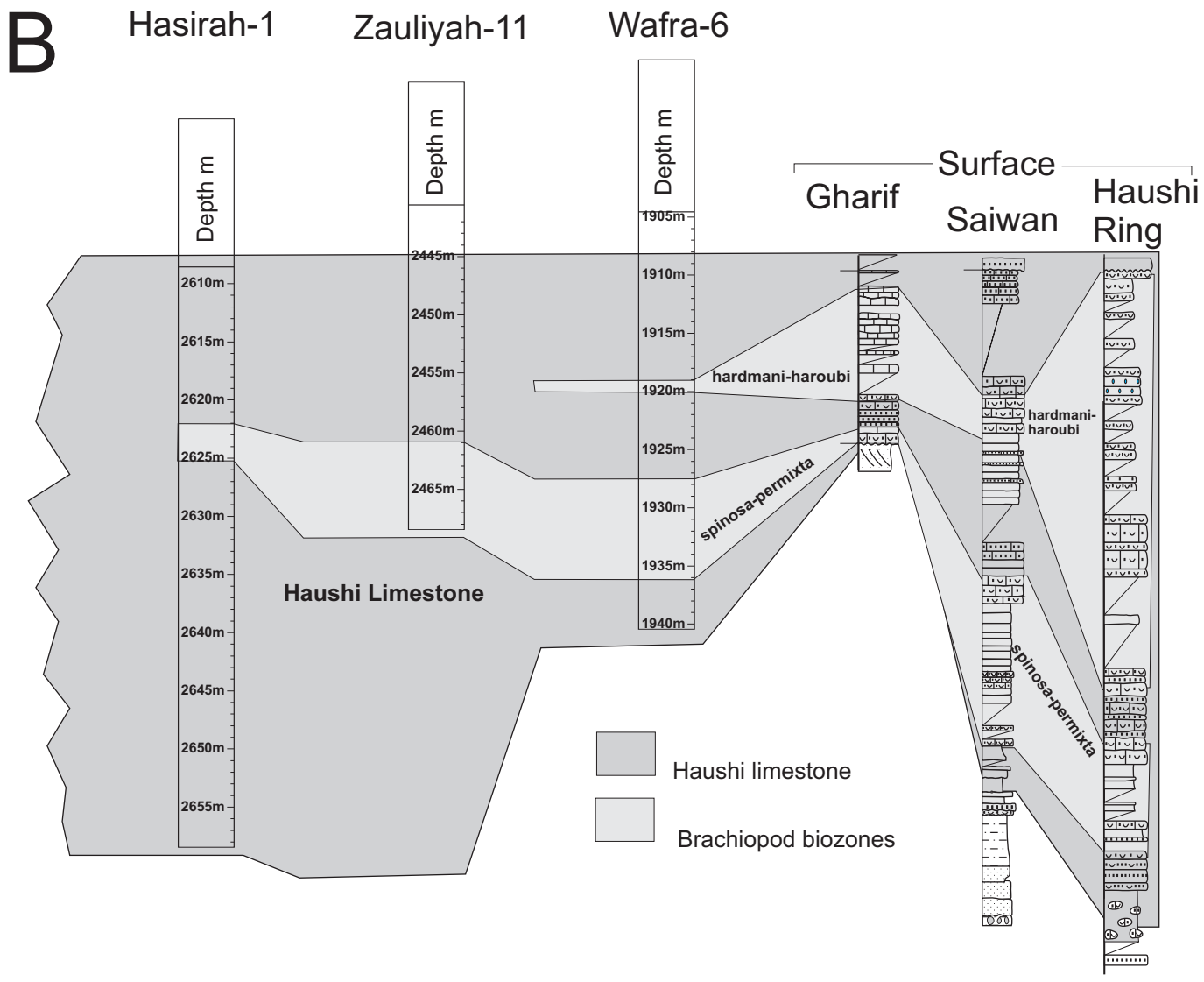

Fig 2

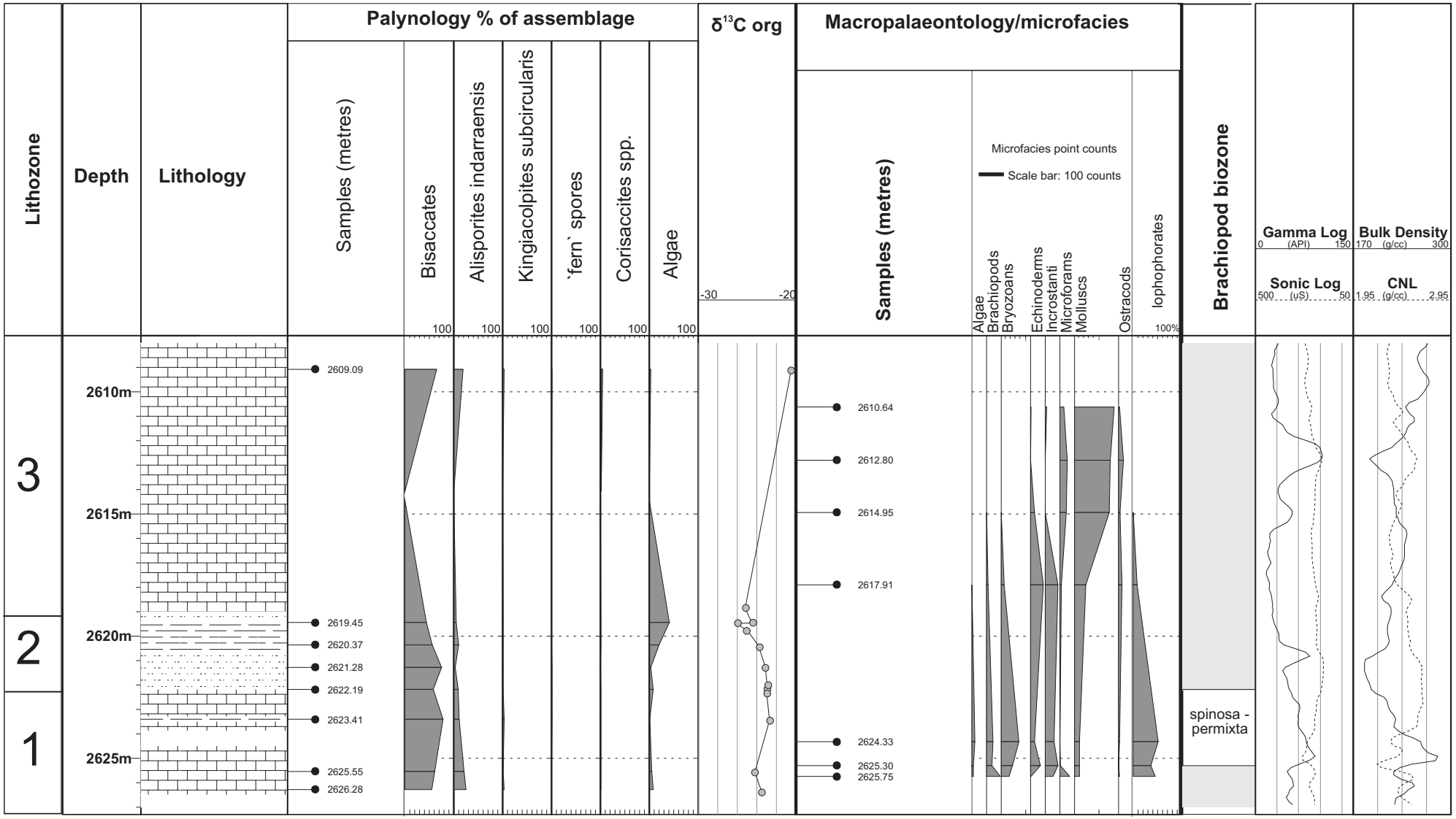
Lithozone
Depth
Lithology
Palynology % of assemblage
Samples (metres)
Bisaccates
Alisporites indarraensis
Kingiacolpites subcircularis
`fern` spores
Corisaccites spp.
Algae
100
δ13C org
-30
-20
Macropalaeontology/microfacies
Samples (metres)
Microfacies point counts
Scale bar: 100 counts
Algae
Brachiopods
Bryozoans
Echinoderms
Incrostanti
Microforams
Molluscs
Ostracods
Iophophorates
100%
Brachiopod biozone
Gamma Log
0 (API) 150
Sonic Log
500 (uS) 50
Bulk Density
170 (g/cc) 300
CNL
1.95 (g/cc) 2.95
3
2
1
2610m
2615m
2620m
2625m
2609.09
2619.45
2620.37
2621.28
2622.19
2623.41
2625.55
2626.28
2610.64
2612.80
2614.95
2617.91
2624.33
2625.30
2625.75
spinosa - permixta

Fig. 3

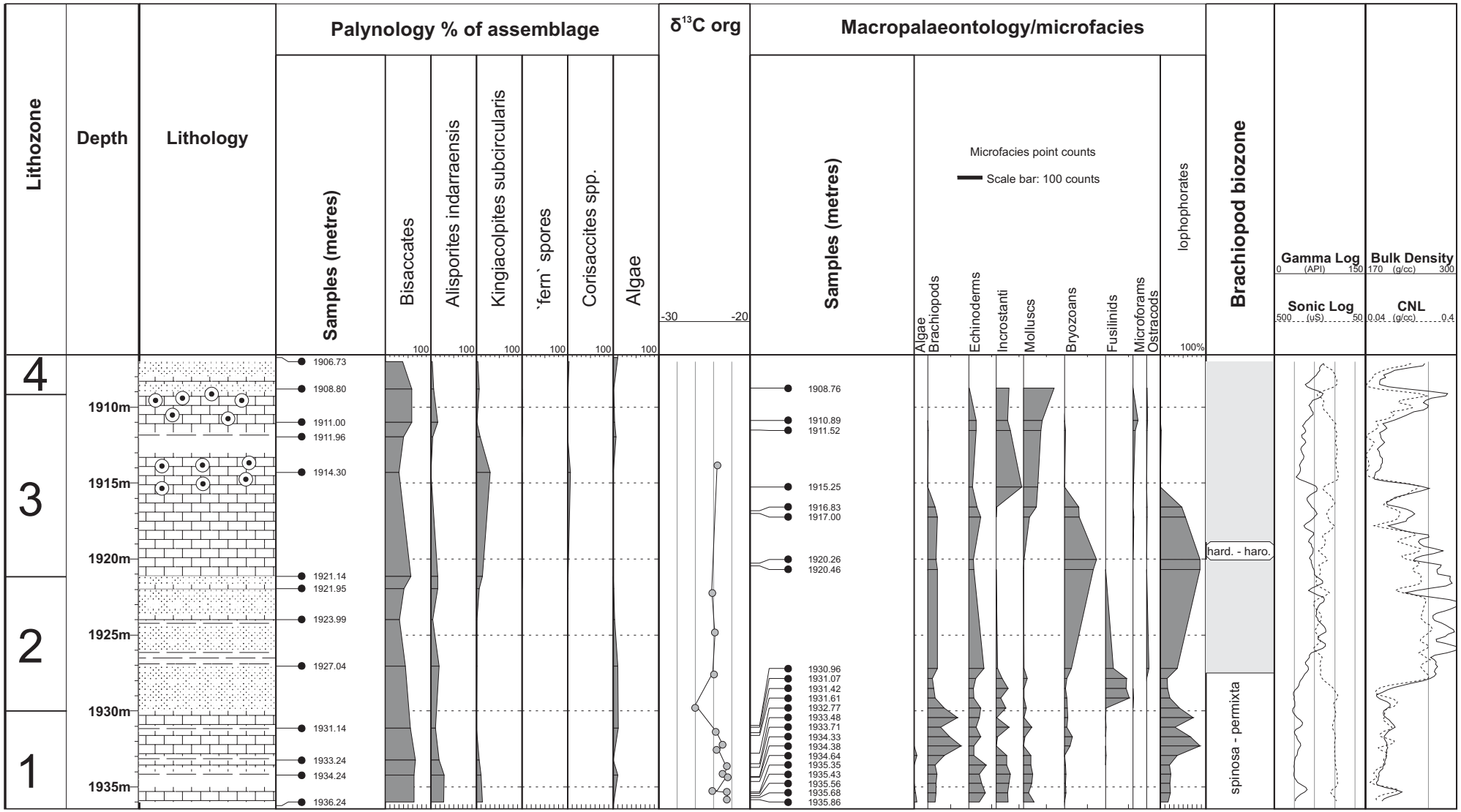
Lithozone
Depth
Lithology
Palynology % of assemblage
Samples (metres)
Bisaccates
Alisporites indarraensis
Kingiacolpites subcircularis
`fern` spores
Corisaccites spp.
Algae
100
δ13C org
-30
-20
Macropalaeontology/microfacies
Samples (metres)
Microfacies point counts
Scale bar: 100 counts
Algae
Brachiopods
Echinoderms
Incrostanti
Molluscs
Bryozoans
Fusilinids
Microforams
Ostracods
lophophorates
100%
Brachiopod biozone
hard. - haro.
spinosa - permixta
Gamma Log
0 (API) 150
Sonic Log
500 (uS) 50
Bulk Density
170 (g/cc) 300
CNL
0.04 (g/cc) 0.4
4
3
2
1
1910m
1915m
1920m
1925m
1930m
1935m
1906.73
1908.80
1911.00
1911.96
1914.30
1921.14
1921.95
1923.99
1927.04
1931.14
1933.24
1934.24
1936.24
1908.76
1910.89
1911.52
1915.25
1916.83
1917.00
1920.26
1920.46
1930.96
1931.07
1931.42
1931.61
1932.77
1933.48
1933.71
1934.33
1934.38
1934.64
1935.35
1935.43
1935.56
1935.68
1935.86

Fig 4

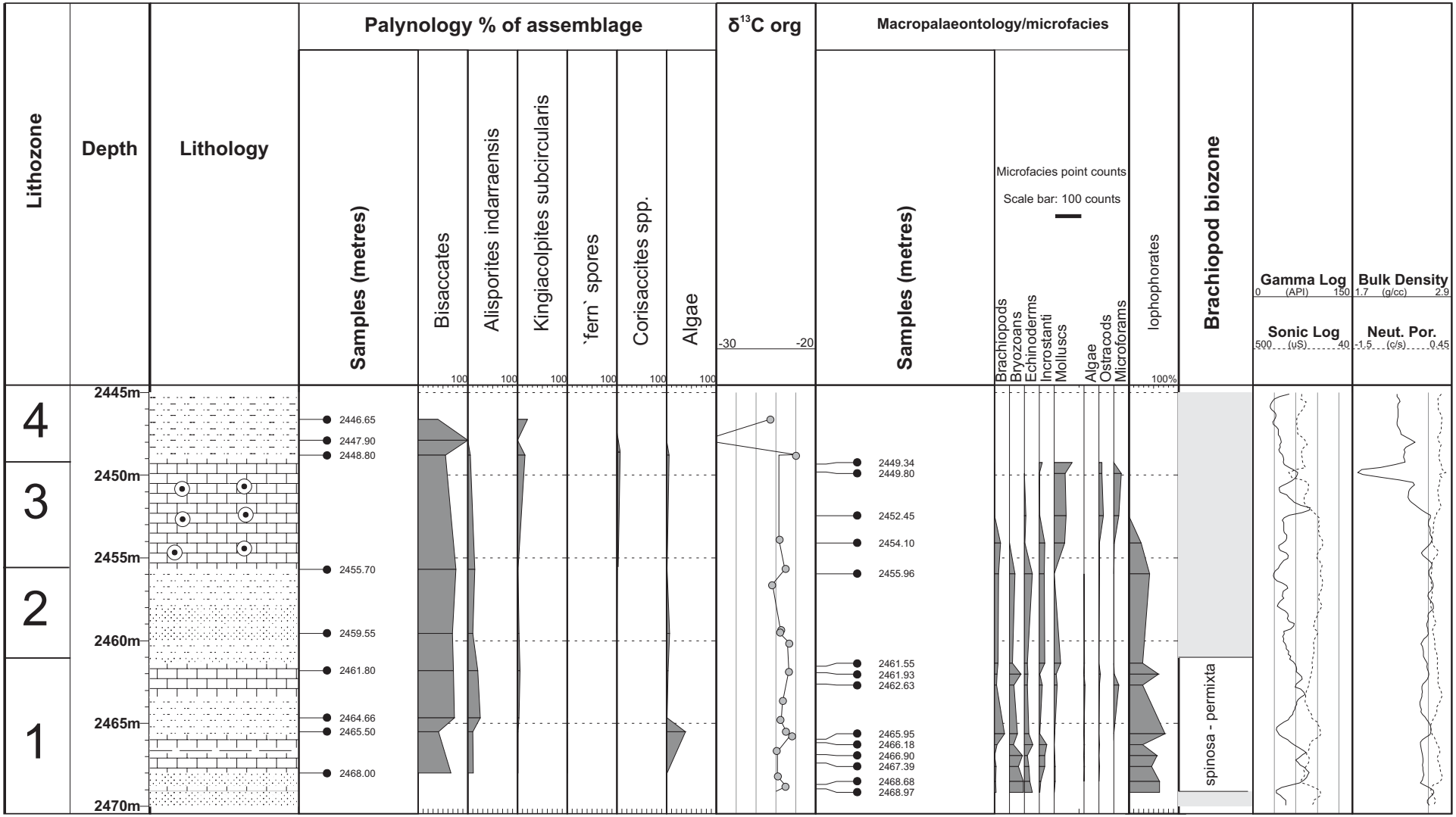
Lithozone
Depth
Lithology
Palynology % of assemblage
Samples (metres)
Bisaccates
Alisporites indarraensis
Kingiacolpites subcircularis
`fern` spores
Corisaccites spp.
Algae
100
δ13C org
-30
-20
Macropalaeontology/microfacies
Samples (metres)
Microfacies point counts
Scale bar: 100 counts
Brachiopods
Bryozoans
Echinoderms
Incrostanti
Molluscs
Algae
Ostracods
Microforams
Iophophorates
100%
Brachiopod biozone
spinosa - permixta
Gamma Log
0 (API) 150
Sonic Log
500 (uS) 40
Bulk Density
1.7 (g/cc) 2.9
Neut. Por.
-1.5 (c/s) 0.45
4
3
2
1
2445m
2450m
2455m
2460m
2465m
2470m
2446.65
2447.90
2448.80
2455.70
2459.55
2461.80
2464.66
2465.50
2468.00
2449.34
2449.80
2452.45
2454.10
2455.96
2461.55
2461.93
2462.63
2465.95
2466.18
2466.90
2467.39
2468.68
2468.97

Fig 5

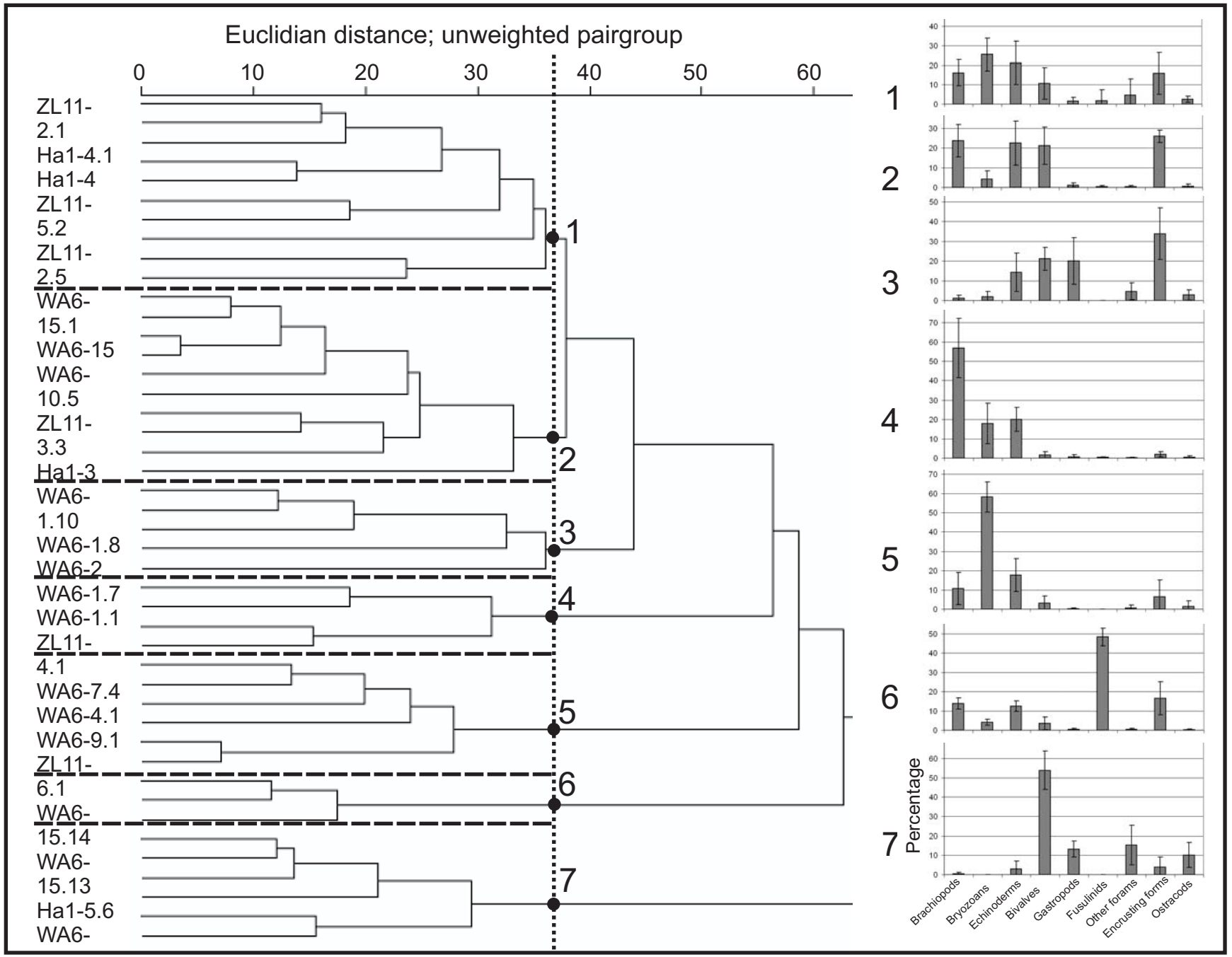
Euclidian distance; unweighted pairgroup
0
10
20
30
40
50
60
ZL11-2.1
Ha1-4.1
Ha1-4
ZL11-5.2
ZL11-2.5
WA6-15.1
WA6-15
WA6-10.5
ZL11-3.3
Ha1-3
WA6-1.10
WA6-1.8
WA6-2
WA6-1.7
WA6-1.1
ZL11-4.1
WA6-7.4
WA6-4.1
WA6-9.1
ZL11-6.1
WA6-15.14
WA6-15.13
Ha1-5.6
WA6-
1
2
3
4
5
6
7
Percentage
Brachiopods
Bryozoans
Echinoderms
Bivalves
Gastropods
Fusulinids
Other forams
Encrusting forms
Ostracods

Fig 6

Figure 7

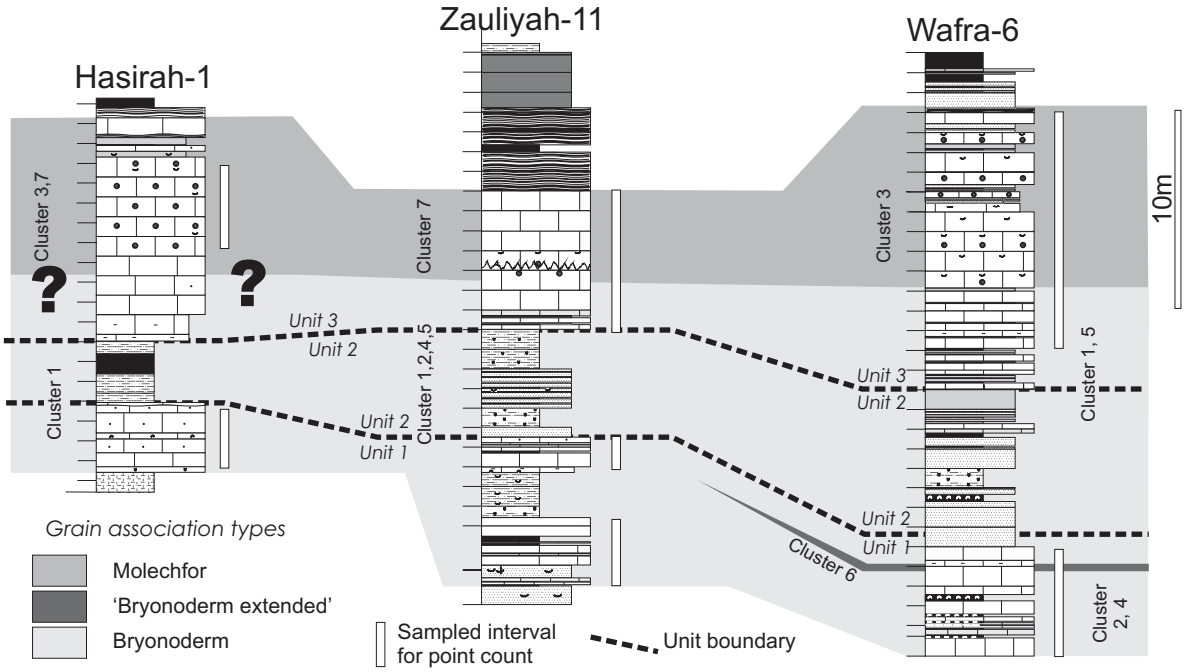

Fig 7

Figure 8

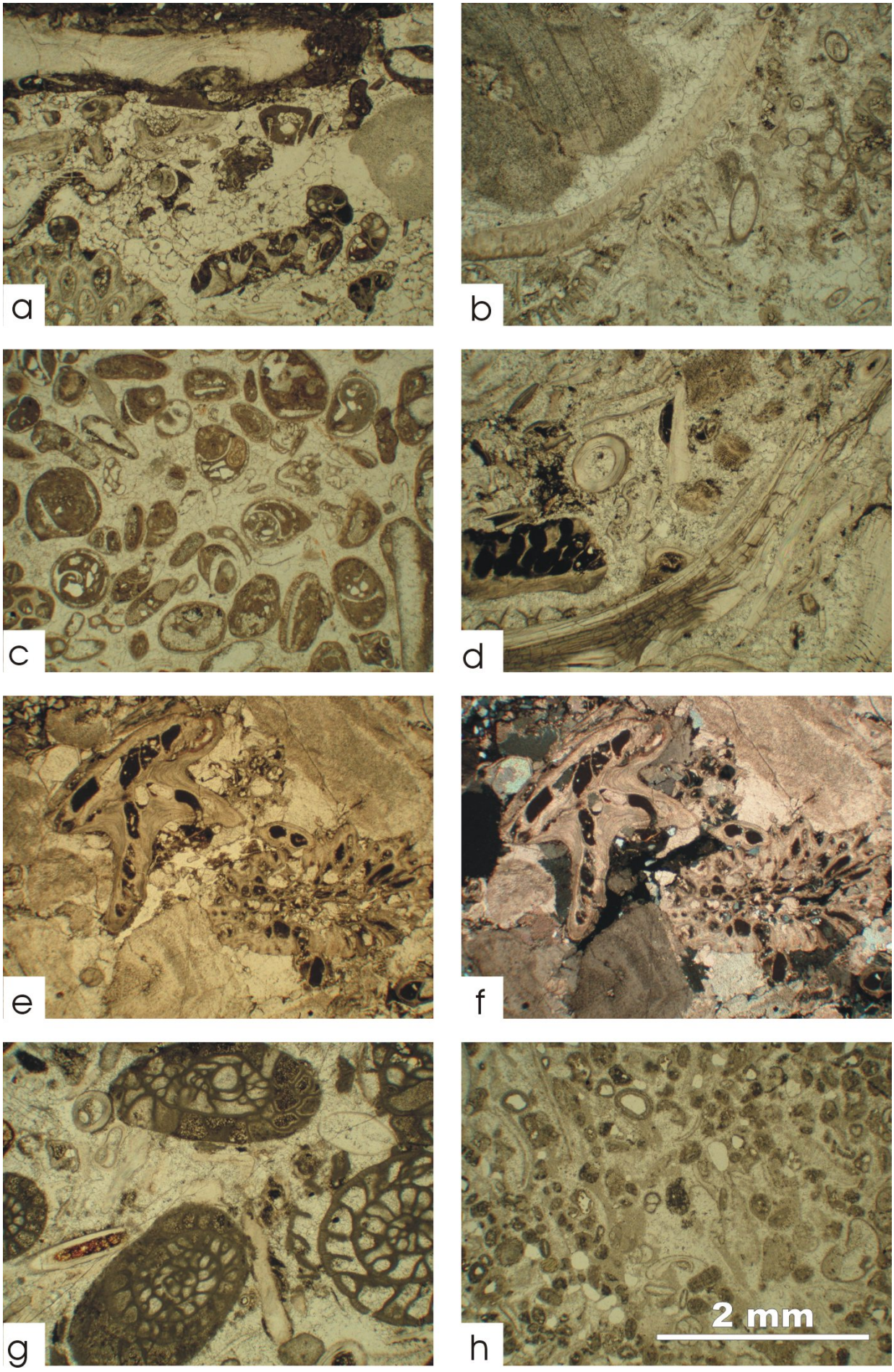

Fig 8

Figure 9

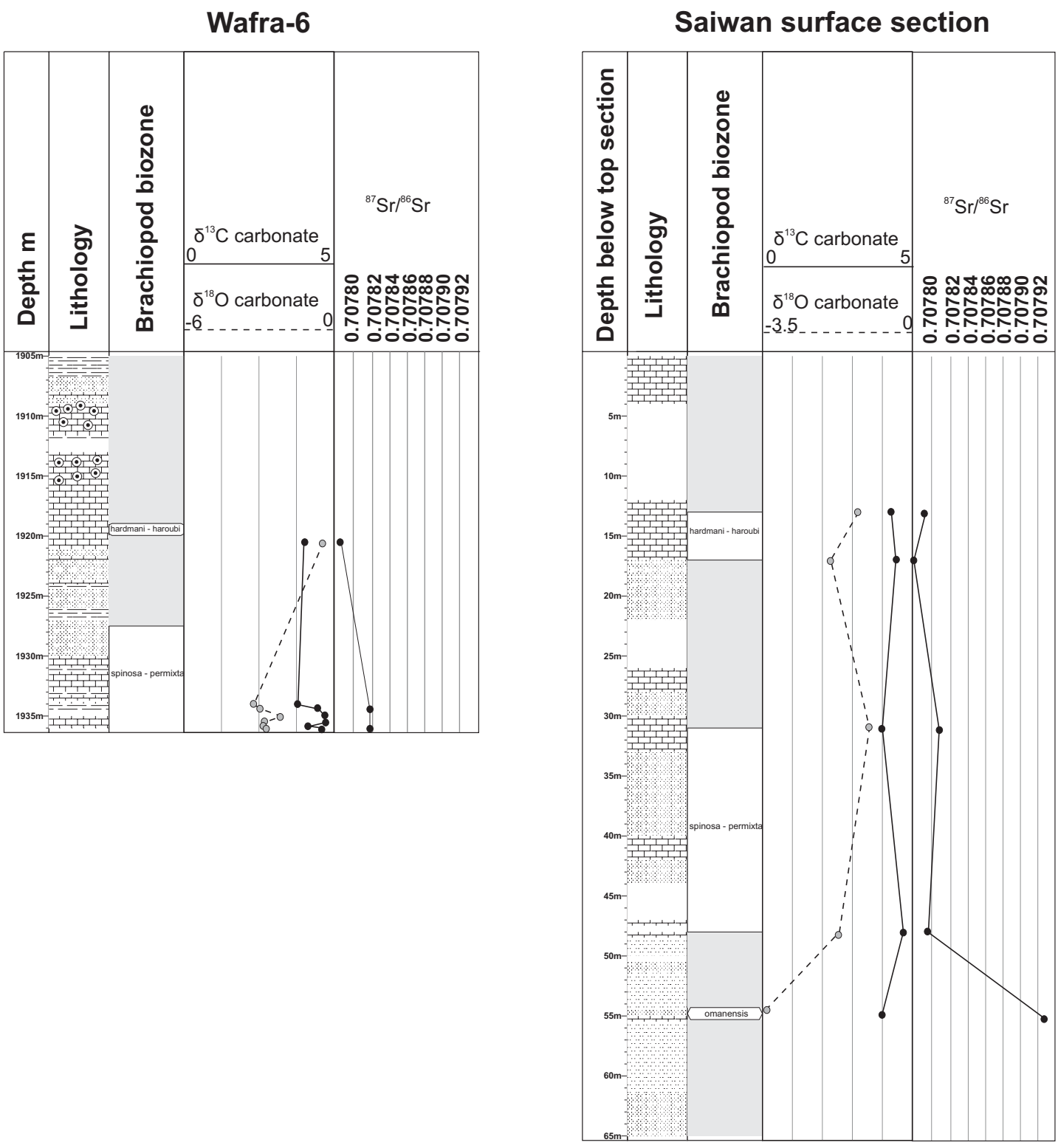

Fig. 9

Figure 10

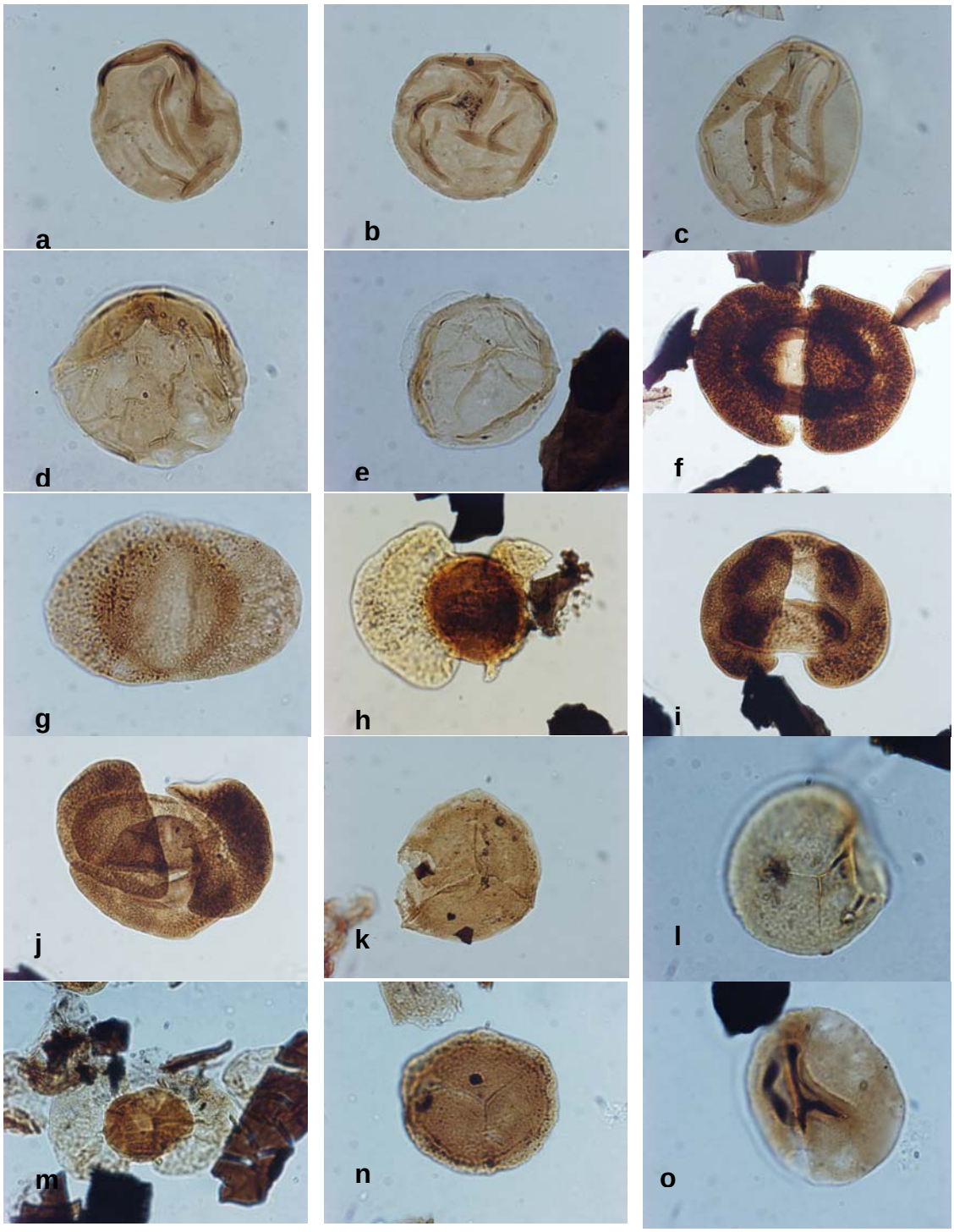

Fig 10

Figure 11

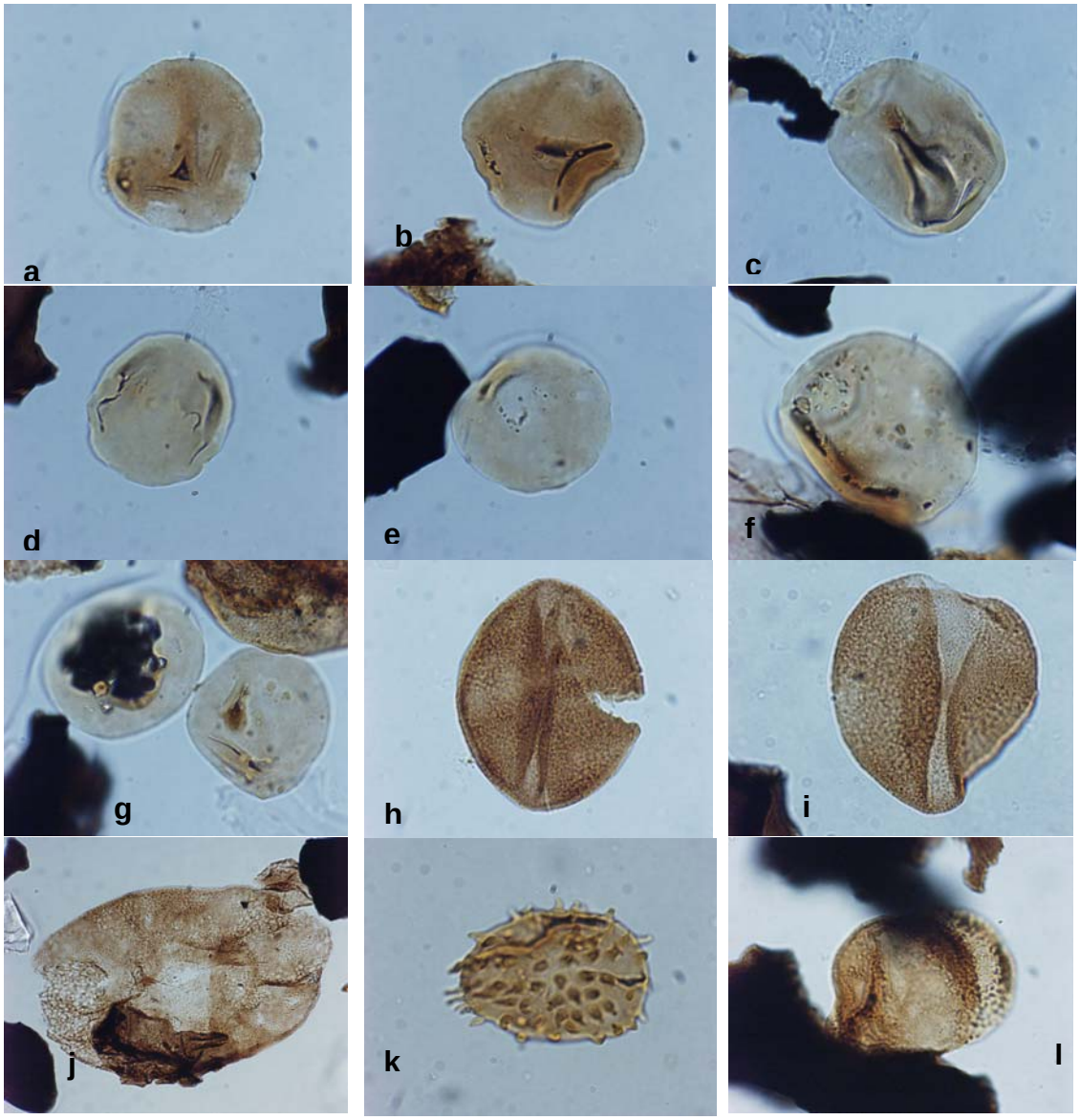

Fig 11

Figure 12

Fig 12

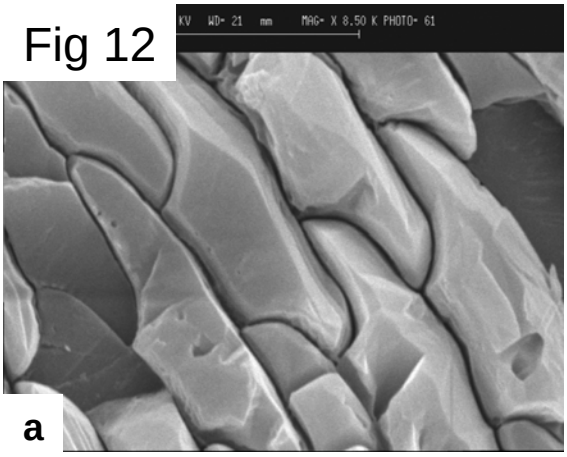

a

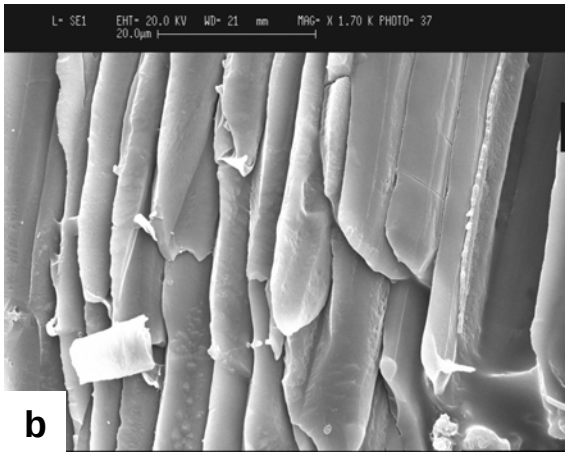

b

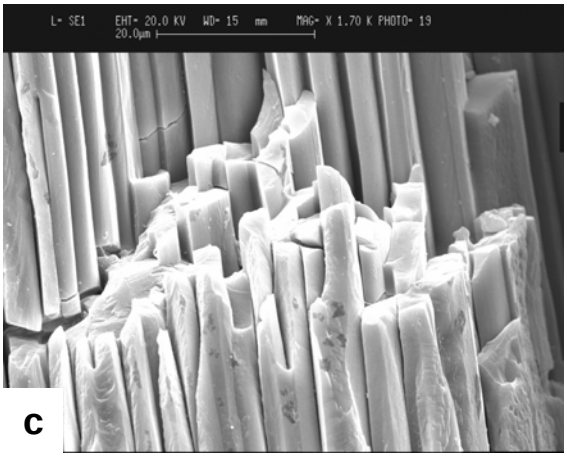

c

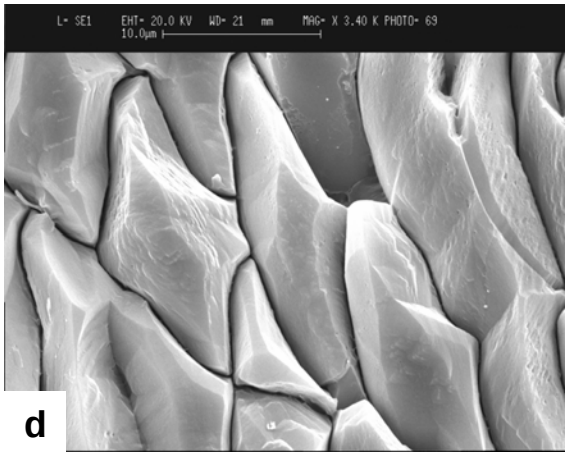

d

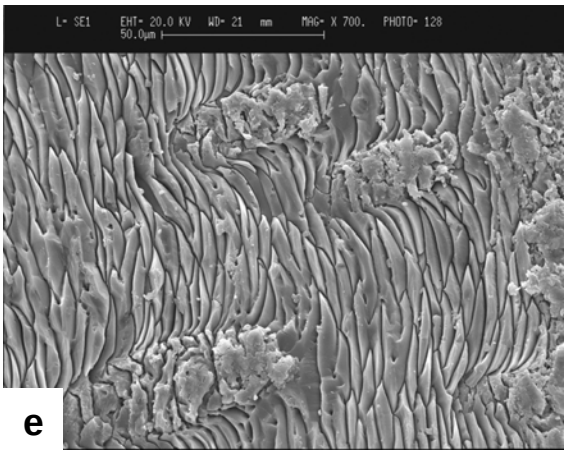

e

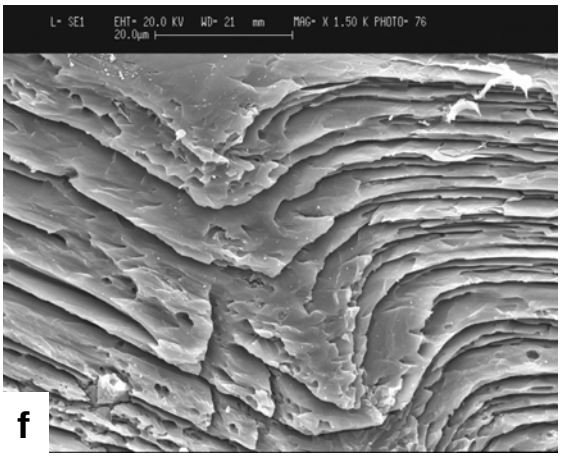

f

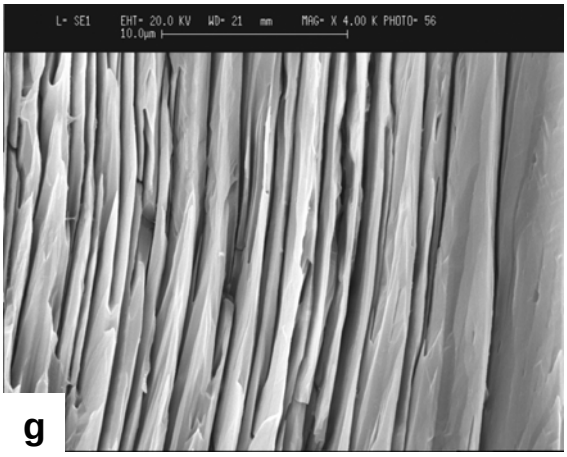

g

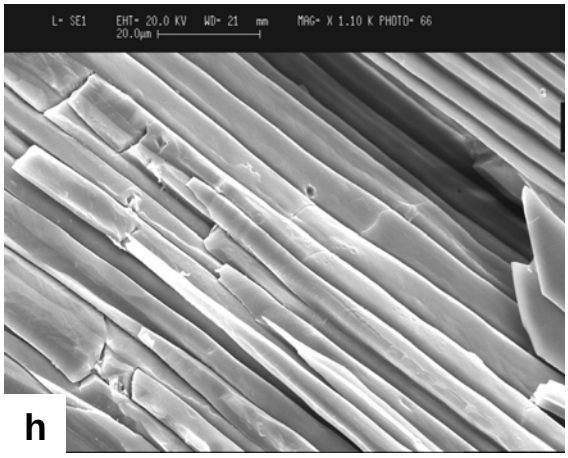

h

Figure 13

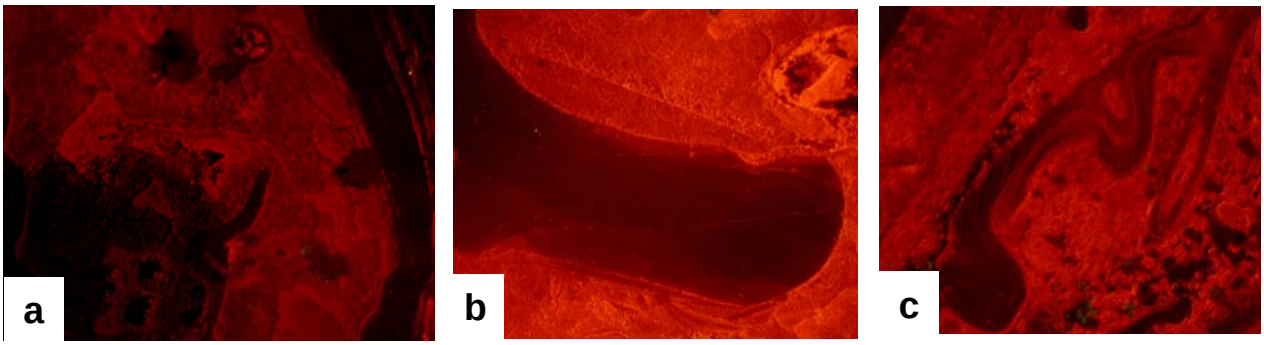

Fig. 13

Table 1

Click here to download Table: Table 1.pdf

Classes	Feeding strategy	Nutrient	Palaeobathymetry	Substrate
Brachiopods	Impingement feeders	Moderate to high	Not indicative	Soft to hard
Bryozoans	Impingement feeders	Moderate to high	Not indicative	Hard
Crinoids	Collision feeders	Normal, constant	Not indicative	hard
Molluscs	Filter feeders & deposit feeders	Normal, constant	Not indicative	soft
Foraminifera (excl. fusulinids)	Filter feeders	Not indicative	Not indicative	soft
Fusulinids	Filter feeders & photosymbiosis	Low	Euphotic zone	soft
Encrusting organisms	Various	Low to high	Not indicative	hard
Ostracods	Filter feeders	High	Not indicative	soft
Calcareous algae	Photosynthesis	Low to high	Euphotic zone	soft to hard

Table 1